iScience

CellPress
OPEN ACCESS

Article

Bacterial Quorum Sensing Molecules Promote Allergic Airway Inflammation by Activating the Retinoic Acid Response

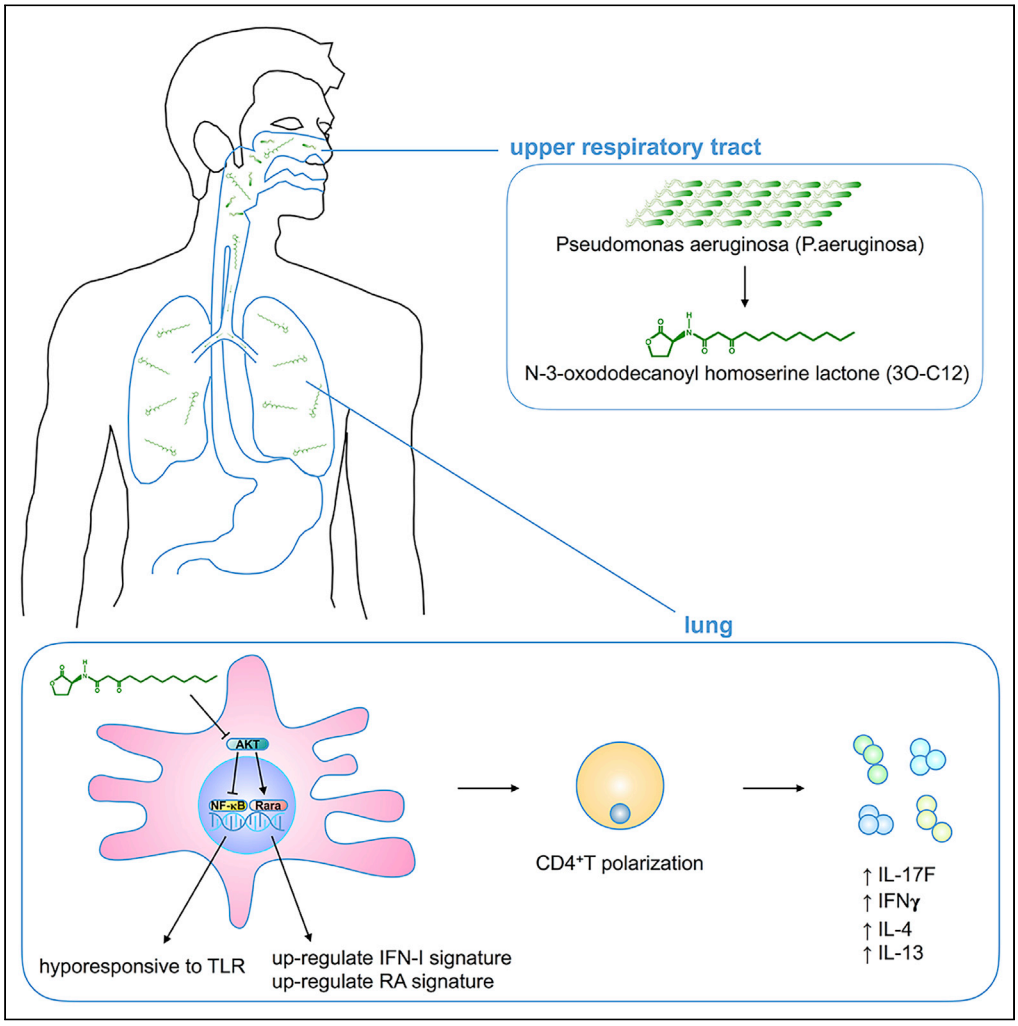

Renlan Wu, Xingjie Li, Ning Ma, ..., Hongmei Tang, Zhigang Liu, Zongde Zhang

zongdez@swmu.edu.cn

HIGHLIGHTS

Acyl homoserine lactones (AHLs) exacerbate allergic airway inflammation

AHLs induce IgE and IgG1 production

AHLs activate the RARE response in dendritic cells

AHLs inhibit AKT phosphorylation

Wu et al., iScience 23, 101288
July 24, 2020
https://doi.org/10.1016/j.isci.2020.101288

iScience

CellPress
OPEN ACCESS

Article

Bacterial Quorum Sensing Molecules Promote Allergic Airway Inflammation by Activating the Retinoic Acid Response

Renlan Wu,[1,4,5] Xingjie Li,[1,3,5] Ning Ma,[1,5] Xiufeng Jin,[1] Xiefang Yuan,[1] Chen Qu,[4] Hongmei Tang,[1] Zhigang Liu,[2] and Zongde Zhang[1,3,4,6,*]

SUMMARY

IgE and IgG1 production in the type 2 immune response is the characteristic feature of an allergic reaction. However, whether bacterial molecules modulate IgE and IgG1 production remains obscure. Here, we demonstrate that the bacterial quorum sensing molecules acyl homoserine lactones (AHLs) induce IgE and IgG1 production by activating the RARE (retinoic acid response element) response in dendritic cells (DCs) *in vivo*. DC-specific knockout of the retinoic acid transcriptional factor Rara diminished the AHL-stimulated type 2 immune response *in vitro*. AHLs altered DC phenotype, upregulated OX40L and IFN-I signature, and promoted T helper 2 cell differentiation *in vitro*. Finally, AHLs activated the RARE response by inhibiting AKT phosphorylation *in vitro*, as the AKT agonists IGF-1 and PDGF abolished the effect of AHLs on the RARE response. This study demonstrates a mechanism by which AHLs drive allergic airway inflammation through activating retinoic acid signaling in DCs.

INTRODUCTION

The prevalence of allergic diseases has increased significantly over the past decades. It has been suggested that "allergic diseases could be prevented by infection, exposure, or colonization of microorganisms in the neonatal period" (Bisgaard et al., 2011; Fyhrquist et al., 2014; Lambrecht and Hammad, 2017; Smits et al., 2016; Strachan, 1989). However, it has also been demonstrated that specific bacterial infection or colonization is a risk factor for food allergies and asthma (Huang and Boushey, 2015; Savage et al., 2018). This paradox reveals the differential role of microbes in shaping the allergic response of the host. There is evidence that exposure to farm dust enriched with bacterial endotoxin can reduce the severity of asthma (Schuijs et al., 2015). Furthermore, gut flora metabolite short-chain fatty acids decrease the circulating level of immunoglobulin E (IgE) and thus ameliorate allergic lung inflammation (Cait et al., 2018). However, whether bacteria-derived molecules can promote allergic reactions remains elusive.

The bacterium *Pseudomonas aeruginosa* causes a wide range of opportunistic infections among immunocompromised patients and is also a commensal bacteria that colonizes the human gut and upper respiratory tract (Huang et al., 2011; Okuda et al., 2010; Stoodley and Thom, 1970). *P. aeruginosa* has been found in patients with asthma (Huang et al., 2011; Li et al., 2017), and its colonization in a patient with chronic rhinosinusitis was correlated with an oncoming attack of asthma (Cleland et al., 2013; Zhang et al., 2015). Furthermore, persistent colonization of *P. aeruginosa* is associated with a positive skin prick test reaction to multiple allergens (Clarke et al., 1981; Pitcher-Wilmott et al., 1982). The mechanisms by which *P. aeruginosa* provokes allergic reactions have not been determined yet.

One specific characteristic of *P. aeruginosa* is to use diffusible acyl homoserine lactones (AHLs) as quorum sensing molecules for inter- and intra-species communication (Khajanchi et al., 2011; Miyairi et al., 2006; Passador et al., 1993; Tang et al., 1996). One of the AHLs, N-3-oxododecanoyl homoserine lactone (3O-C12), has been demonstrated to possess immunomodulatory properties such as inhibition of lymphocyte proliferation and downregulation of T helper 1 (Th1) cytokine interleukin (IL)-12 production (Telford et al., 1998). This suggests that 3O-C12 may promote Th2 differentiation in the allergic response.

[1]Inflammation & Allergic Diseases Research Unit, Affiliated Hospital of Southwest Medical University, Luzhou, Sichuan 646000, China

[2]State Key Laboratory of Respiratory Disease for Allergy at Shenzhen University, Shenzhen University School of Medicine, Shenzhen 518060, China

[3]The School of Basic Medical Sciences, Southwest Medical University, Luzhou, Sichuan 646000, China

[4]Model Animal Research Center, Nanjing University, Nanjing 210061, China

[5]These authors contributed equally

[6]Lead Contact

*Correspondence: zongdez@swmu.edu.cn

https://doi.org/10.1016/j.isci.2020.101288

Dendritic cells (DCs) are the most effective antigen-presenting cells. After engulfing an antigen, DCs stimulate CD4+ T cells toward Th1 or Th2 differentiation, which leads to specific antibody production in B cells. Previously, we demonstrated that commensal fungi in the gut are essential for maintaining DC retinoic acid (RA) signaling in lymphoid tissue (Zhang et al., 2016). However, overgrowth of commensal fungi in the gut induced M2 macrophage polarization and exacerbated pulmonary allergic reactions (Kim et al., 2014; Skalski et al., 2018). Furthermore, it has been demonstrated that RA can promote M2 macrophage polarization (Chen et al., 2019; Vellozo et al., 2017) and boost Th2 cytokine production (Dawson et al., 2008; Lovett-Racke and Racke, 2002), which are critical for class switching recombination of IgE and IgG1. These studies imply a link between microorganisms, RAs, and allergic reactions. Furthermore, another study has indicated that intestinal microbiota can modulate RA signaling in intestinal epithelial cells (Bhattacharya et al., 2016). These findings led us to investigate whether bacteria-derived 3O-C12 could modulate RA signaling in DCs, which may contribute to the type 2 immune response.

Allergen-specific IgE and IgG1 production is the hallmark of allergic diseases. T helper 2 (Th2) cytokines such as IL-4 and IL-13 are required for class switching recombination of IgE and IgG1 (Gould and Sutton, 2008). After engulfing antigens, DCs can stimulate CD4+ T cells toward Th2 differentiation by multiple mechanisms involving the DC surface protein OX40L (Flynn et al., 1998; Ito et al., 2005; Kaisar et al., 2018; Ohshima et al., 1998); transcription factors IRF4, IL-10, and IL-33 (Gao et al., 2013; Williams et al., 2013); and the recently identified DC-intrinsic type I interferon signature (Connor et al., 2017; Janss et al., 2016; Webb et al., 2017). However, whether bacteria-derived molecules engage these DC genes and prime CD4+ T cell Th2 differentiation remains incompletely understood.

In this study, we demonstrate that the bacterial quorum sensing molecule 3O-C12 stimulates IgE and IgG1 production by provoking the DC RARE (retinoic acid response element) response. 3O-C12 inhibits Toll-like receptor (TLR)-induced DC maturation but activates type I interferon and OX40L by the RA signal transcription factor retinoic acid receptor α (Rara). This study sheds light on the important roles of bacterial diffusible AHL molecules in promoting host allergic reactions via DC RA signaling.

RESULTS

3O-C12 Stimulates Allergic Lung Inflammation

The production of specific IgE and IgG1 in the type 2 immune response is characteristic of allergic diseases. Colonization of *P. aeruginosa* is highly correlated with the development of an allergic reaction (Clarke et al., 1981; Cleland et al., 2013; Zhang et al., 2015). To test the possibility that *P. aeruginosa*-derived 3O-C12 promotes allergen-specific antibody production, wild-type C57BL/6 mice were immunized with OVA and 3O-C12 for 3 weeks (Figure 1A). 3O-C12 was derived from the gram-negative bacteria *P. aeruginosa*. The outer membrane of gram-negative bacteria is largely made of lipopolysaccharide (LPS), which suggests that 3O-C12 may activate an immune response together with LPS. Indeed, LPS has been used as an adjuvant in studying DC priming of the Th1-Th2 response (Gao et al., 2013). To mimic the genuine biological scenario, we also added LPS to OVA and 3O-C12 for mice immunization. 3O-C12 alone or with LPS significantly increased serum OVA-specific IgE and IgG1, slightly increased OVA-specific IgA and IgG2b, and moderately decreased OVA-specific IgG2a, IgG2c, and IgM production (Figure 1B). 3O-C12 alone or with LPS changed the DC phenotype and promoted IL-4, IL-5, and IL-13 production in $CD4^+$ T cells (Figures S1E and S1F). Next, we examined whether 3O-C12 administration can increase allergic lung inflammation in a mouse model of asthma. 3O-C12 increased the total number of infiltrated cells (Figure 1D), including eosinophils (Figure 1E) in the bronchoalveolar lavage fluid; the cytokine response of $CD4^+$T cells (Figure S1B); and airway inflammation (Figure 1C). 3O-C12 changed the surface marker expression of spleen-derived DCs (Figure S1A). Intranasal transfer of OVA-loaded, 3O-C12-activated bone marrow-derived dendritic cells (BMDCs) induced OVA-specific IgE (Figure S1C), higher levels of cytokines by splenic $CD4^+$T cells (Figure S1D), and airway inflammation (Figure 1F). These data reveal the stimulative role of 3O-C12 on allergic lung inflammation.

3O-C12-Activated DCs Are Hyporesponsive to TLR Stimulation and Induce the RARE Response

Next, we investigated whether bacteria-derived 3O-C12 could modulate RA signaling in DCs, which may contribute to the type 2 immune response. We used RA reporter transgenic mice that bear a β-galactosidase (LacZ) reporter under the control of a RARE (Figure 2A), and thus β-galactosidase activity could be measured by DDAO galactoside (DDAOG) to DDAO conversion. We stimulated BMDCs and

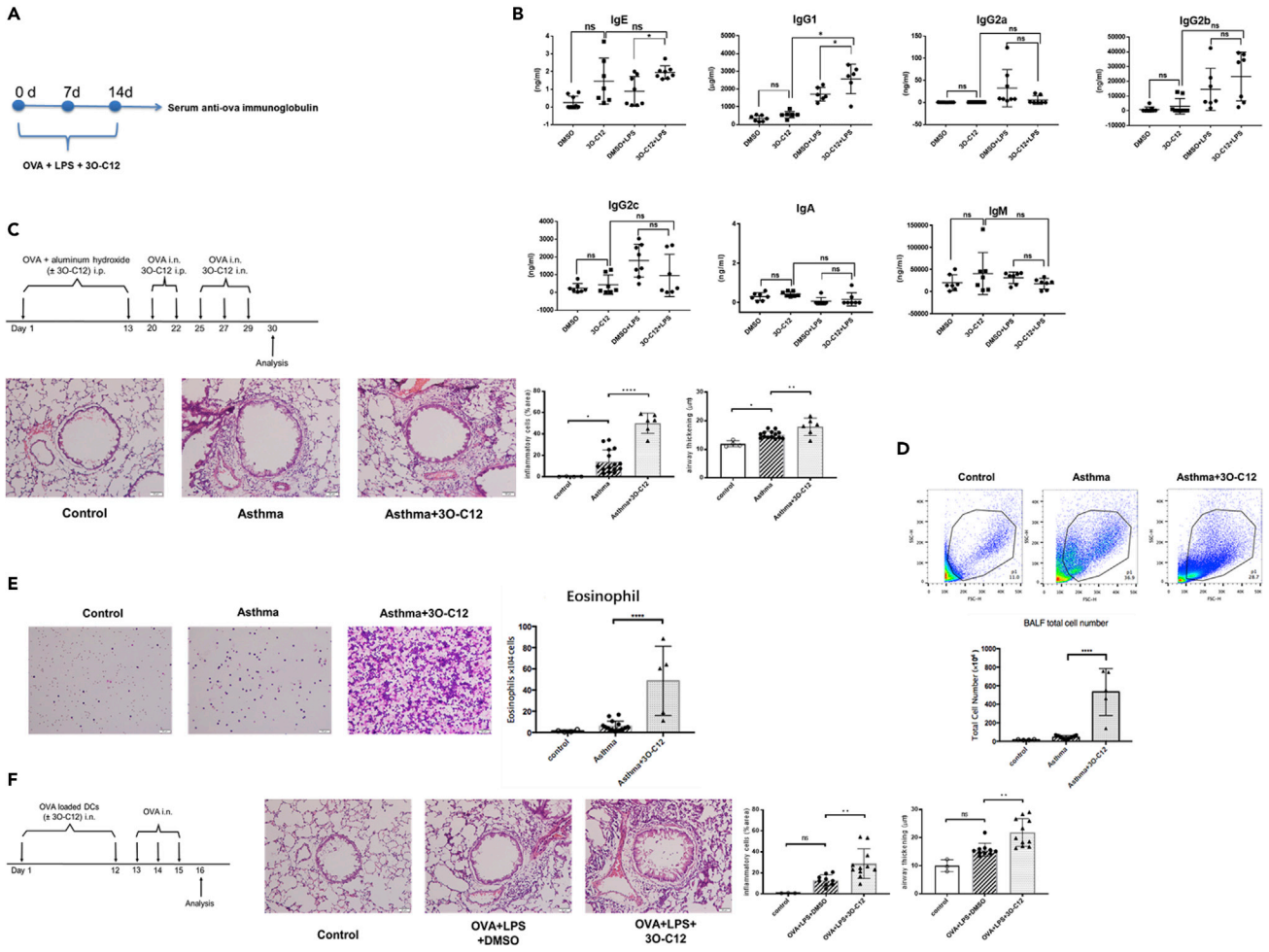

Figure 1. 3O-C12 Stimulates OVA-Specific IgE and IgG1 Production and Enhances Allergic Lung Inflammation

(A) Graphical representation of mouse immunization.

(B) Wild-type C57BL/6 mice (6–8 weeks, male and female) were subcutaneously immunized with OVA (50 μg/mouse) + LPS (0.5 μg/mouse) with or without 3O-C12 (250 μg/mouse) every week for 3 weeks; incomplete Freund adjuvant was used as a vehicle. Mouse serum was collected; OVA-specific IgE, IgG1, IgG2a, IgG2c, IgM, IgA, and IgG2b were analyzed with ELISA. Results are representative of three independent experiments.

(C–E) (C) BALB/c mice were divided into three groups: control (n = 4), asthma (n = 15), and asthma + 3O-C12 (n = 6). The mice were intraperitoneally (i.p.) injected on days 1 and 13 with OVA (50 μg) and aluminum hydroxide (2 mg). On days 20 and 22, the mice were intranasally (i.n.) challenged with OVA (40 μg) and i.p. administered with or without 3O-C12 (500 μg). On days 25, 27, and 29, the mice were i.n. challenged with OVA (40 μg) and i.n. administered with or without 3O-C12 (50 μg). One day after the last OVA challenge, mice were sacrificed and assessed for lung histology (scale bar, 50 μm) (C) and bronchoalveolar lavage fluid (BALF) total cell number (D) and eosinophil number (E).

(F) BMDCs from C57BL/6 mice were stimulated by OVA (200 μg/mL) and LPS (100 ng/mL) overnight, with or without 3O-C12 (10 μM). BMDCs were transferred i.n. to recipients (C57BL/6 mice) (n = 3 in control group; n = 10 in OVA + LPS + DMSO group; n = 11 in OVA + LPS + 3O-C12 group) on days 1 and 12. Each recipient was challenged with 40 μg OVA i.n. on days 13, 14, and 15. One day after the last OVA challenge, mice were sacrificed and assessed for lung histology (scale bar, 50 μm). The statistical quantification (inflammatory cells and airway thickening) of Figures 1C and 1F was analyzed by ImageJ software. Data are presented as mean ± SD; p values were calculated using the two-tailed Student's t test. Data that did not exhibit a normal distribution were analyzed using the nonparametric Kruskal-Wallis test with Dunn's post hoc test. *$p < 0.05$, **$p < 0.01$, ***$p < 0.001$, ****$p < 0.0001$; n.s., not significant.

spleen-derived DCs (spDCs) isolated from the transgenic mice with 3O-C12. BMDCs exposed to 3O-C12 exhibited increased DDAO fluorescence (Figure 2B). However, the DC activation markers CD40, CD80, and CD86 were reduced after exposure to 3O-C12 (Figure 2C). The maturation marker CD80 was downregulated on spDCs exposed to 3O-C12 (Figure 2D). It was reported that the hyporesponse of DCs to TLR stimulation may involve the Th2 response (Gao et al., 2013). Here, we provide evidence that 3O-C12 could inhibit LPS-induced BMDC activation, as the surface markers ICAM1, CD40, CD80, and CD86 were downregulated and cytokine IL-6 and tumor necrosis factor (TNF)-α production was reduced (Figure 2E). The

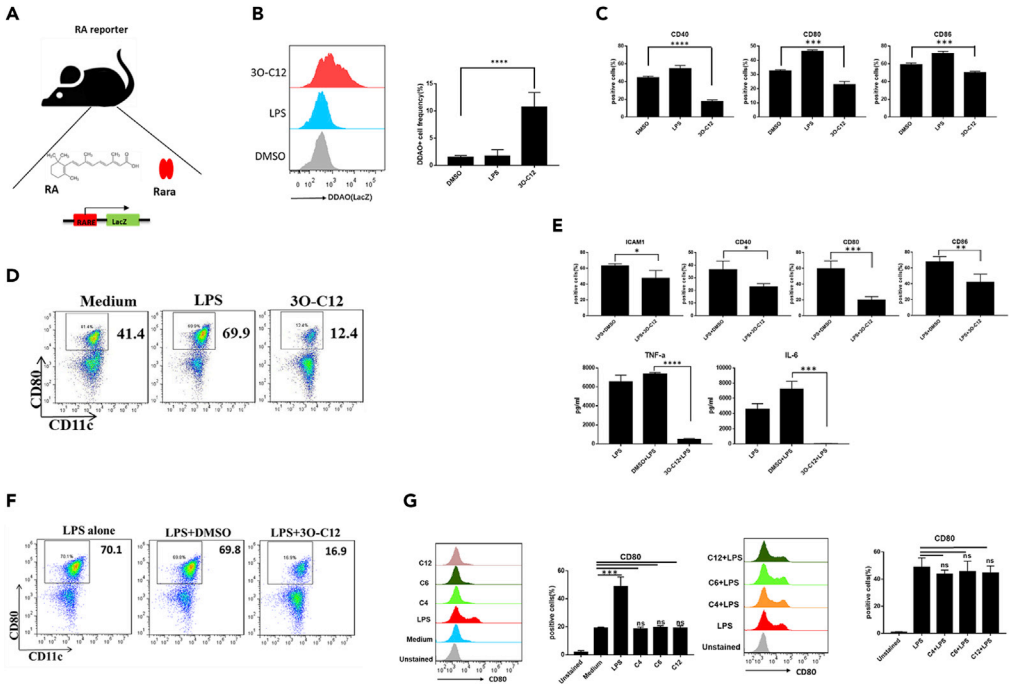

Figure 2. 3O-C12 Activates the RARE Response

(A) Graphical representation of the working model of RA reporter mice.

(B) BMDCs (5–7 days) cultured from RA reporter mice were stimulated with 3O-C12 (10 μM) or LPS (100 ng/mL) for 1–2 h and incubated with DDAOG (10 μM). DDAO fluorescence was analyzed by flow cytometry. Data are representative of three independent experiments (n = 5–7).

(C) BMDCs (5–7 days) cultured from RA reporter mice were stimulated with 3O-C12 (10 μM) or LPS (100 ng/mL) overnight. Expression levels of CD40, CD80, and CD86 were determined by flow cytometry; cells were gated on CD11c-positive cells. Data are representative of three independent experiments (n = 5–7).

(D) DC Magnetic-activated cell sorting (MACS) isolated from the spleen of C57BL/6 mice were stimulated with LPS (100 ng) or 3O-C12 (10 μM) or were unstimulated (medium). CD80 expression was determined by flow cytometry. Data are representative of three independent experiments (n = 5–7).

(E) BMDCs (5–7 days) cultured from RA reporter mice were stimulated with LPS (100 ng/mL) overnight, with or without 3O-C12 (10 μM). Expression levels of ICAM1, CD40, CD80, and CD86 were determined by flow cytometry. Cytokine levels of IL-6 and TNF-α were evaluated by ELISA. Data are representative of three independent experiments (n = 5–7).

(F) DC MACS isolated from the spleen of C57BL/6 mice were stimulated with LPS (100 ng) with or without 3O-C12 (10 μM) overnight. CD80 expression was determined by flow cytometry. Data are representative of three independent experiments (n = 5–7).

(G) BMDCs (5–7 days) cultured from RA reporter mice were stimulated with C4 (10 μM), C6 (10 μM), and C12 (10 μM) alone or plus LPS. CD80 expression was determined by flow cytometry. Data are representative of three independent experiments (n = 5–7).

Data are presented as mean ± SD; p values were calculated using two-tailed Student's t test. *$p < 0.05$, **$p < 0.01$, ***$p < 0.001$, ****$p < 0.0001$; n.s., not significant.

effect of 3O-C12 was similar on both spDCs and BMDCs, namely, a reduced expression of CD80 after LPS stimulation (Figure 2F). However, the quorum sensing molecules C4, C6, and C12 neither inhibited DC maturation nor blocked LPS-induced CD80 expression (Figure 2G). Furthermore, we investigated whether other TLR pathways could be blocked by 3O-C12. First, we evaluated the TLR expression level during BMDC development. TLR-3, TLR-4, and TLR-7 were upregulated and TLR-5 was downregulated on day 6 (Figure S2A). 3O-C12 inhibited TLR ligands 1–7- and TLR ligand 9-induced DC activation (Figure 3A). High-dose exposure to 3O-C12 caused DC apoptosis, whereas lower doses (5 and 10 μM) did not (Figure 3B). A high dose of 3O-C12 (25 μM) induced B and T cell apoptosis *in vitro* (Figure S2B), consistent with a previous study (Song et al., 2019). We further used the multiple cytokine detection system MILLIPLEX Multiplex Assays, which demonstrated that 3O-C12 changed chemokine expression. The chemokine CCL22 was secreted mainly by DCs, and its expression depended on nuclear factor (NF)-κB activation

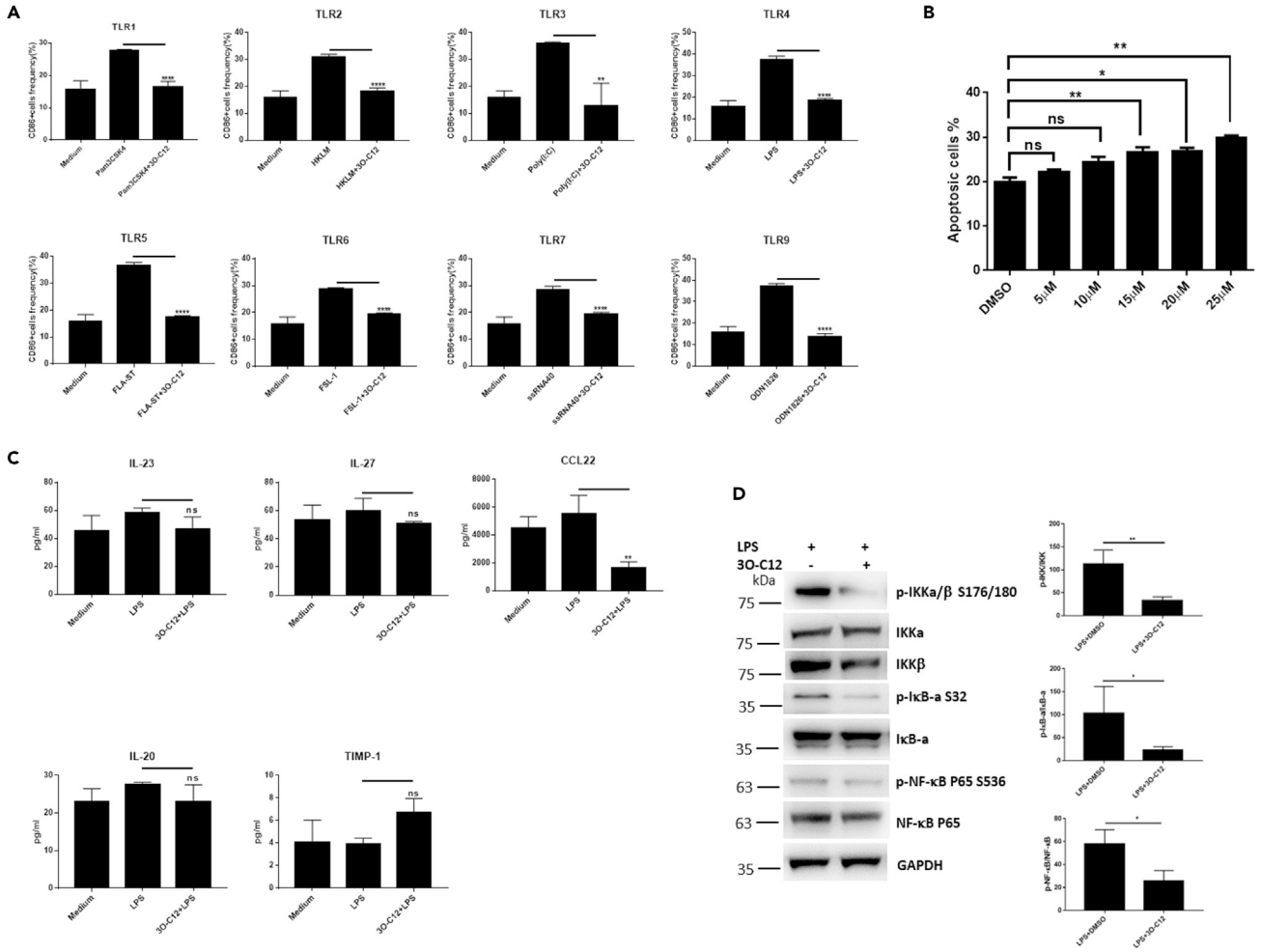

Figure 3. 3O-C12 Inhibits TLR-Induced DC Activation

(A) BMDCs (5–7 days) cultured from C57BL/6 mice were stimulated with different TLR ligands with or without 3O-C12 (10 μM) overnight. CD86-positive cells were estimated by flow cytometry. Data are representative of three independent experiments (n = 5–7).

(B) BMDCs (5–7 days) cultured from C57BL/6 mice were incubated with different doses of 3O-C12 for 12 h; annexin V-positive cells were determined by flow cytometry. Data are representative of three independent experiments (n = 5–7).

(C) BMDCs (5–7 days) cultured from C57BL/6 mice were unstimulated (medium) or stimulated with LPS or LPS + 3O-C12 (5 μM) overnight. Cytokines were determined by MILLIPLEX Multiplex Assays. Data are representative of three independent experiments (n = 5–7).

(D) BMDCs (5–7 days) cultured from C57BL/6 mice were incubated with LPS plus 3O-C12 (10 μM) for 3 h. Cells were collected and lysed and activation of the NF-κB pathway was determined by western blot (n = 4).

Data are presented as mean ± SD; p values were calculated using the two-tailed Student's t test. *p < 0.05, **p < 0.01, ****p < 0.0001; n.s., not significant.

and was significantly downregulated (Figure 3C). In contrast, IL-20, IL-27, IL-23, and TIMP-1 expression levels were not changed (Figure 3C). Moreover, 3O-C12 could block NF-κB pathway activation in DCs (Figure 3D), consistent with a previous report (Kravchenko et al., 2008). Downregulation of CCL22 by 3O-C12 may be due to the reduced activation of the NF-κB pathway in DCs. Collectively, these results suggest that 3O-C12 changes DC phenotype by inhibiting TLR signaling and activating a RA response.

The Specific Chemical Structure of AHLs Determines the RARE Response in DCs

The quorum sensing molecule AHL family includes numerous chemical molecules that differ in their R-group side-chain length. Chain lengths vary from 4 to 18 carbon atoms and in the substitution of a carbonyl at the third carbon. To pinpoint which chemical structure of AHL could activate RA signaling in DCs, 13 AHLs were screened (Table S1). Only the long chain (R-group side-chain lengths of more than 12 carbon

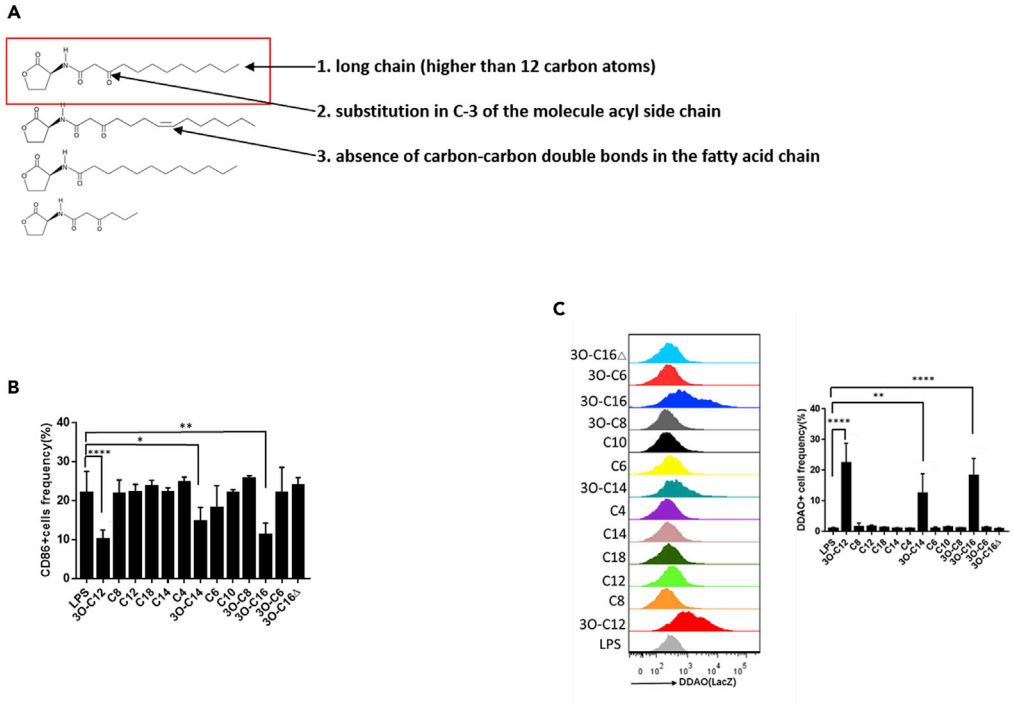

Figure 4. The Chemical Structure of AHLs Determines the RARE Response

(A) The RARE response depends on the chemical structure of AHLs with three characteristics.

(B) BMDCs (5–7 days) cultured from C57BL/6 mice were stimulated with LPS (100 ng/mL) with or without AHLs (10 μM) overnight. CD86-positive cells were estimated by flow cytometry. Data are representative of three independent experiments (n = 5–7).

(C) BMDCs (5–7 days) cultured from RA reporter mice were stimulated with AHLs (10 μM) or LPS (100 ng/mL) for 1–2 h and incubated with DDAOG (10 μM) for 1–2 h. DDAO fluorescence was analyzed by flow cytometry. Data are representative of three independent experiments (n = 5–7).

Data are presented as mean ± SD; p values were calculated using the two-tailed Student's t-test. *$p < 0.05$, **$p < 0.01$, ****$p < 0.0001$; n.s., not significant.

atoms) and C-3 substitution in the acyl side chain exhibited the ability to activate RA signaling (Figures 4A and 4C); the only exception was 3O-C16 △ with one carbon-carbon double bond in the fatty acid chain. The result was correlated with DC inhibition and downregulation of CD86 expression by these AHLs (Figure 4B). These data identified the chemical structure of AHLs that is responsible for activating RA signaling in DCs (Figures 4A and 4C).

3O-C12 Activates the DC RARE Response through the Inhibition of AKT Signaling

To investigate the mechanism by which 3O-C12 activates the DC RARE response, we assessed the T2R38 taste receptor previously reported as a sensing receptor for 3O-C12. We investigated agonist binding to the T2R38 receptor as well as induced phospholipase C activation (Lee et al., 2012). Activating T2R38 with the agonists 6PTU (6-n-propylthiouracil) and NP (N-phenylthiourea) or inhibiting phospholipase C activation with U73122 neither changed the RARE response nor downregulated CD86 in DCs (Figure 5A). This indicated that T2R38 is not linked to the DC RARE response. AKT signaling is indispensable for TLR activation (Joung et al., 2011; Lee et al., 2003; Park et al., 2006). AKT also suppresses the transactivation of Rara in a subset of non-small cell lung cancer cells (Srinivas et al., 2006). We reasoned that 3O-C12 may regulate AKT signaling involved in the DC RARE response. We found that 3O-C12 could quench AKT activation in DCs with decreased phosphorylation of AKT (s-473) and GSK-3b, a downstream target that is phosphorylated by AKT (Figure 5B). Other AHLs such as 3O-C14 and 3O-C16, which could stimulate a RARE response in DCs, also exhibited the ability to quench AKT phosphorylation (Figure 5C). Furthermore, activation of the PI3K pathway through insulin-like growth factor 1 (IGF-1) and platelet-derived growth factor (PDGF) abolished the 3O-C12-activated DC RARE response (Figure 5D). These data indicate that 3O-C12 activates the DC RARE response through the inhibition of AKT signaling.

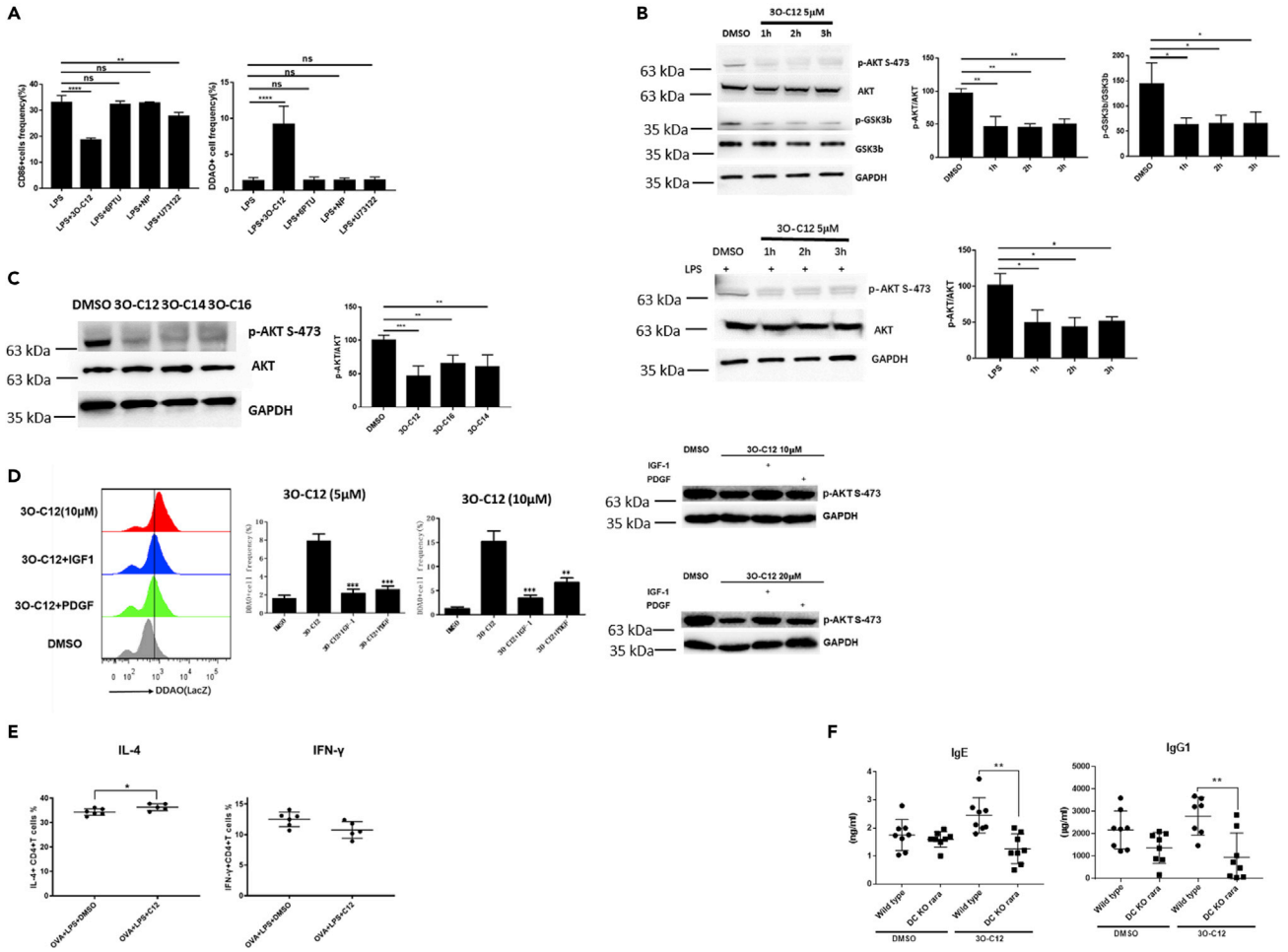

Figure 5. 3O-C12 Activates the RARE Response by Disrupting AKT Signaling

(A) BMDCs (5–7 days) cultured from RA reporter mice were stimulated with LPS alone (100 ng/mL) or LPS plus 3O-C12 (33 μM), 6PTU (100 uM), NP (100 uM), or U73122 (10 μM) overnight and incubated with DDAOG (10 μM) for 1–2 h. DDAO fluorescence and CD86 expression were analyzed by flow cytometry. Data are representative of three independent experiments.

(B and C) (B) BMDCs (5–7 days) cultured from C57BL/6 mice were incubated with 3O-C12 (10 μM) for 1–3 h or (C) LPS plus 3O-C12. Cells were collected and lysed, and AKT phosphorylation was determined by western blot. Results are representative of three independent experiments.

(D) BMDCs (5–7 days) cultured from RA reporter mice were stimulated with 3O-C12 (5 μM and 10 μM) or 3O-C12 plus IGF-1 (200 ng/mL) and PDGF (40 ng/mL) for 1–2 h and incubated with DDAOG (10 μM) for 1–2 h. DDAO fluorescence was analyzed by flow cytometry. AKT phosphorylation was determined by western blot. Data are representative of three independent experiments.

(E) BMDCs (5–7 days) cultured from C57BL/6 mice were loaded with OVA (100 μg/mL), incubated with LPS, or LPS+3O-C12 (10 μM) for 1–3 h; naive OT-II cells were added and co-cultured for 5 days. IL4- and IFN-γ-positive cells were determined by flow cytometry. Data are representative of three independent experiments.

(F) 6- to 8-week-old male and female CD11ccre^{+}Rara$^{fl/fl}$ mice (DC KO Rara) and littermate control CD11ccre^{-}Rara$^{fl/fl}$ mice (wild-type) were subcutaneously immunized with OVA (50 μg/mice) + LPS (0.5 μg/mice) with or without 3O-C12 (250 μg/mouse) every week for 3 weeks. Mouse serum was collected, and OVA-specific IgE and IgG1 were analyzed by ELISA. Results are representative of three independent experiments.

Data are presented as mean ± SD; p values were calculated using the two-tailed Student's t test. *p < 0.05, **p < 0.01, ***p < 0.001, ****p < 0.0001; n.s., not significant.

3O-C12-Induced Th2 Differentiation Depends on the Transcription Factor Rara

We next investigated whether 3O-C12 could induce DCs to prime CD4+ T cells toward Th2 differentiation. Isolated OT-II cells were co-cultured with DCs in the presence of the OVA antigen. After exposure to 3O-C12, DCs stimulated CD4+ T cells toward Th2 differentiation, as IL-4^{+} cells were upregulated (Figure 5E) and produced high levels of IL-5 and IL-13 (Figure S2C).

To confirm if a lack of RA signaling in DCs impairs IgE and IgG1 production *in vivo*, we established DC-specific Rara gene knockout (KO) mice ($CD11c^{cre}Rara^{fl/fl}$), as Rara is the dominant RA signaling transcription factor in DCs (Galvin et al., 2013). After immunization with OVA plus LPS and 3O-C12, we found that the DC-specific KO of the Rara gene (DC KO rara) significantly reduced OVA-specific IgE and IgG1 production in mice (Figures 5F and S2E). However, DC KO rara did not change basal immunoglobulin levels (Figure S2F). Furthermore, DC KO rara impaired CD4+ T cell Th2 differentiation in 3O-C12-activated BMDCs *in vitro* and *in vivo* (Figures S2D and S2H). Collectively, these data indicate that the quorum sensing molecule 3O-C12 boosts the allergic type 2 immune response by activating RA signaling in DCs.

To gain further insight into the mechanism of 3O-C12-activated DCs and to identify the cellular targets of 3O-C12 that are involved in CD4+T cell Th2 differentiation, we isolated mRNA from 3O-C12-activated and control DCs and subjected it to Illumina transcriptome sequencing. Transcripts with p value <0.05 between the two groups were graphed by functions. Among the genes differentially expressed, RA signatures, including Cyp26b1, RALDH1 (Aldh1a1), and RALDH3 (Aldh1a3), were upregulated in 3O-C12-activated DCs (Figures 6A and 6B), consistent with the result that 3O-C12 could stimulate a RARE response in DCs. Unexpectedly, the type I interferon (IFN-I) signatures, including Ifit1, Mx1, and Oasl1, were upregulated in 3O-C12-activated DCs (Figures 6A and 6B). The IFN-I signature has been well defined as a critical player in DCs for the initiation of the Th2 response (Connor et al., 2017; Janss et al., 2016; Webb et al., 2017). The IFN-I signature result was confirmed by qPCR (Figure S3A). Chemokines and chemokine receptors were also altered in 3O-C12-stimulated DCs (Figure S3B). Next, we confirmed that the 3O-C12-induced RA and IFN-I signatures were dependent on the transcription factor Rara, as 3O-C12 was unable to upregulate these two signatures in BMDCs from DC Rara KO mice (Figures S3C and 6C).

OX4OL has been indicated as a critical molecule in Th2 cell induction primed by DCs. Here, we found that 3O-C12 with or without LPS could enhance the expression of OX4OL in DCs (Figure 6D). Immunization of mice with OVA/3O-C12 could stimulate OX40L expression on DCs *in vivo*, but not on B or T cells in the drain lymph node (Figure 6F). Furthermore, we confirmed that 3O-C12 upregulated the IFN-I signature in DCs *in vivo* (Figure 6E), suggesting that 3O-C12 specifically targets DCs.

We observed that LPS could slightly enhance 3O-C12-induced IgE and IgG1 production (Figure 1B). LPS-activated DCs favor Th1 induction by the inhibition of Th2 differentiation via the TNF-α/IL-12 circuit (Bachus et al., 2019). However, in some cases, it has been suggested that LPS can contribute to the severity of Th2 lung inflammation and food allergies (Michel et al., 1996; Rodriguez et al., 2017), which may involve OX40L (Duan et al., 2008) and IFN-I (Pollara et al., 2006). To clarify the synergic role of LPS in the 3O-C12-induced type 2 immune response, we isolated mRNA from LPS- and LPS/3O-C12-activated DCs, which was then subjected to Illumina transcriptome sequencing. Transcripts with p values <0.05 between the two groups were graphed by functions. Compared with LPS alone, LPS plus 3O-C12 upregulated the IFN-I signature, RA signature, and chemokines/chemokine receptors (Figures S4A–S4C), which suggests a vital role of 3O-C12 in the upregulation of these genes. Furthermore, LPS could enhance the effect of 3O-C12 on the IFN-I signature, but mitigated the RA signature compared with 3O-C12 alone (Figure S4E). Fn14 (TNFRSF12A or TweakR), previously reported as a Th2-driven factor (Son et al., 2013), was also upregulated by 3O-C12, observed with RNA sequencing (RNA-seq) (Figure S3C) or qPCR (Figure S4D). Moreover, 3O-C12 enhances the expression of OX40L while reducing the production of IL-12 in LPS-stimulated DCs (Figure S4F). Next, we tested whether 3O-C12 can upregulate the transcriptional factor c-Maf, previously reported as an inhibitor of IL-12 (Homma et al., 2007). However, c-Maf was not changed by 3O-C12 (Figure S4G), which suggests that the inhibitory effect of 3O-C12 on IL-12 is not due to c-Maf induction. Collectively, 3O-C12 stimulates DC upregulation of Th2-driving genes (type I-IFN and OX40L).

DISCUSSION

The high colonization rate of *P. aeruginosa* in allergic patients implies that this bacterium may provoke allergies. In this study, we suggest that structure-specific quorum sensing AHL molecules promote OVA-specific IgE and IgG1 production *in vivo* by activating the RARE response in DCs. Cell-specific deletion of RA transcriptional factor Rara in DCs diminishes AHL-induced IgE and IgG1 production. Moreover, we further found that AHLs activate the RARE response by inhibiting AKT phosphorylation. DC exposure to AHLs inhibits the NF-κB pathway and quenches TLR activation.

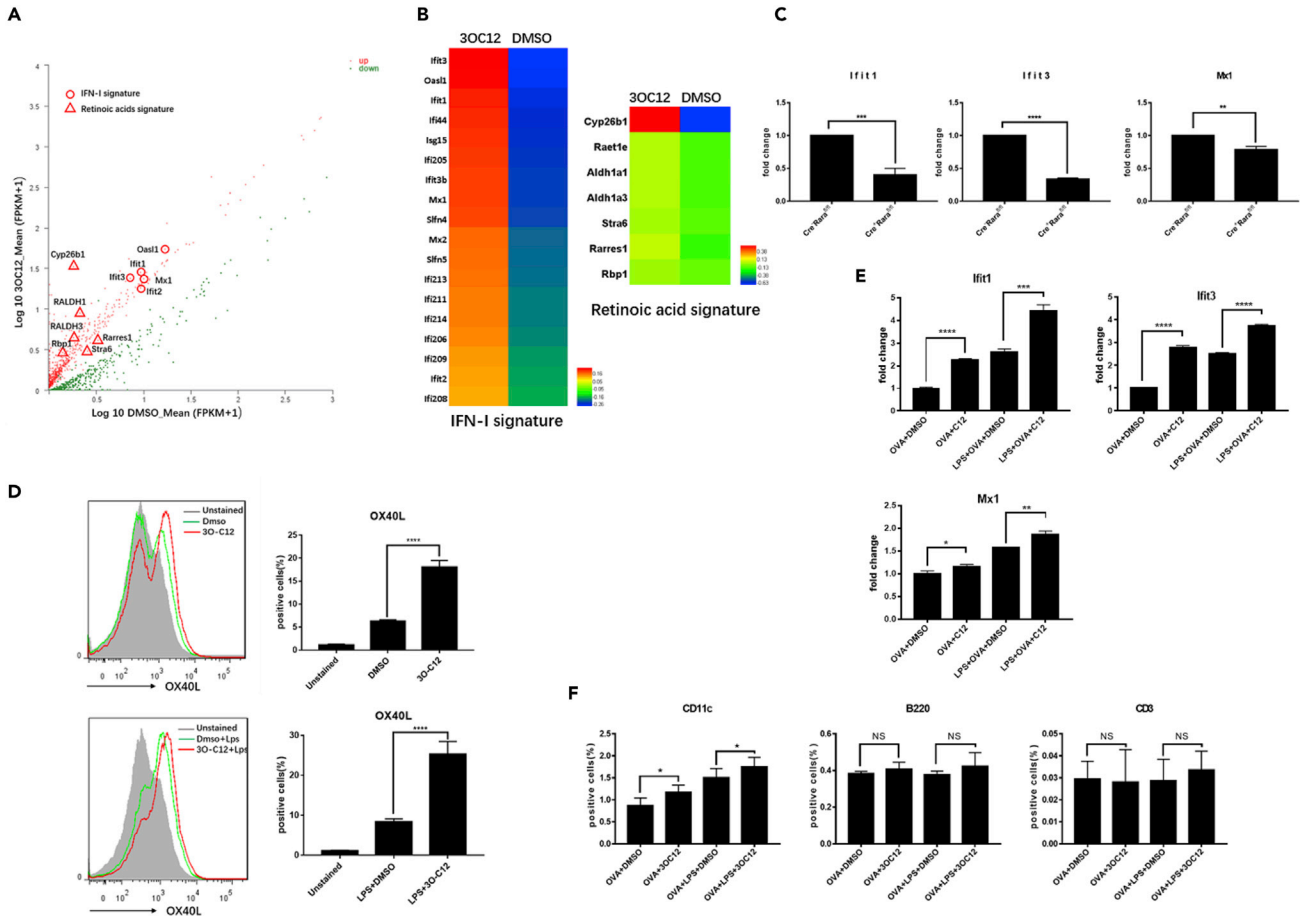

Figure 6. 3O-C12 Stimulates the IFN-I Signature and OX40L

(A and B) RNA sequencing analysis of the gene expression of 3O-C12-activated DCs. (A) Scatterplot of gene expression of FPKM values. (B) Heatmap of FPKM values, IFN-I signature, and RA signature.

(C) The 3O-C12-stimulated IFN-I signature depends on Rara. Gene expression levels were examined by qPCR. Results are representative of two independent experiments.

(D) Fluorescence-activated cell sorting analysis of OX40L in 3O-C12-activated DCs (upper panel) and 3O-C12+LPS-activated DCs (lower panel). Results are representative of four independent experiments.

(E) 3O-C12 stimulates expression of the IFN-I signature in DCs *in vivo*. Results are representative of three independent experiments.

(F) 3O-C12 upregulates OX40L in DCs *in vivo*. Results are representative of two independent experiments (n = 5–7).

p values were calculated using the two-tailed Student's t test. *$p < 0.05$, **$p < 0.01$, ***$p < 0.001$, ****$p < 0.0001$; n.s., not significant.

Quorum sensing is a process of communication among bacteria that allows the coordination of group behavior based on cell density. During bacterial signaling, AHLs are produced within the bacterial cell and released into the environment. Bacteria-derived molecules like TLR and short-chain fatty acids have been demonstrated to inhibit antigenic IgE production, which reflects the basis of the "hygiene hypothesis." In this study, administration of 3O-C12 increased allergic lung inflammation in a mouse model of asthma. The polarization of Th1, Th2, and Th17 cells was observed in the lung, which differs from the effect of 3O-C12 on $CD4^+$T cell Th2 polarization *in vitro*. These interesting differences may be due to the different mouse models *in vitro* and *in vivo*. Intranasal transfer of OVA-loaded, 3O-C12 activated BMDC induced OVA-specific IgE, but not IgG1. This result may reflect the different effect of AHLs on DCs *in vitro* and *in vivo*. Our findings provide a mechanism by which the bacterial quorum sensing molecules AHLs modulate DC signaling, which facilitates IgE and IgG1 production.

RA is synthesized from retinol via two enzymatic reactions, involving first, reversible oxidation of retinol to retinal and then a second oxidation, irreversible metabolism into RA via retinal dehydrogenases (RALDH). DCs from gut-associated lymphoid tissue (GALT) and the draining lymph nodes of the skin and lung

express RALDH, and have the capacity to synthesize RA. In addition to DCs, several nonhematopoietic lineages within GALT, such as epithelia and stromal cells share the capacity to synthesize RA. RAs are essential for immune system development (Zhang et al., 2016) and maintenance of host defense (Hall et al., 2011b). RAs have been demonstrated to stimulate CD4+ T cells for Th2 differentiation. Here, we found that AHLs could stimulate the type 2 immune reaction by inducing the RARE response in DCs. DC-specific KO of Rara reverses the effect of AHLs on OVA-specific IgE and IgG1 production. Cre recombinase is widely used to precisely manipulate genes and chromosomes, but it can also display off-target activity. In this study, CD11c cre^{-} Rara$^{fl/fl}$ mice were used as littermate controls, and we did not add CD11c cre^{+} RARA$^{wt/wt}$ mice as controls.

The AKT pathway is indispensable for TLR activation in DCs. In this study, we illustrated that AHLs inhibit TLR activation, but activate the RARE response by quenching AKT phosphorylation in DCs. Furthermore, we demonstrated that only a long chain (R-group side-chain lengths with more than 12 carbon atoms), absence of carbon-carbon double bonds in the fatty acid chain, and C-3 substitution in the acyl side chain have the ability to activate RA signaling. Stimulation of DCs with IGF-1 and PDGF, two potent agonists of AKT, eliminated the stimulative effect of AHLs on RARE. Our study links AKT signaling and the RARE response with the AHL-induced type 2 immune response. However, the mechanisms of how specific chemical structures of AHLs block AKT phosphorylation need to be further investigated.

AHLs stimulated DCs to be hyporesponsive to TLR. RNA-seq analysis revealed that AHLs induced the IFN-I and RA signatures. This phenotype of AHL-activated DCs resembles a previously reported DC subset involved in Th2 priming (Gao et al., 2013), with a characteristic reduced response to TLR and high expression of Mx1 (IFN-I signature) and Aldh1a2 (RA signature). Furthermore, we confirmed that AHL-stimulated IFN-I and RA signatures both depended on the Rara transcriptional factor. Although the role of Rara in effector CD4+ T cells has been studied (Hall et al., 2011a), it is unclear if it modulates the phenotype of DCs for Th1 or Th2 induction. In this study, we provide evidence that DC-intrinsic Rara can act as a Th2 induction factor.

IL-12 production in DCs induces the differentiation of naive CD4+ T cells to become IFN-γ-producing Th1 cells (Trinchieri, 1994). The impaired production of IL-12 could induce DCs to prime Th2 cells, which may depend on TNF-α. OX40L has been well described as a principal factor in DCs for the induction of Th2 cells. Here, we provide evidence that AHLs upregulate OX40L but downregulate IL-12 in DCs. However, this phenotype may not only depend on Rara but also depend on the inhibitory role of AHLs on TNF-α.

Collectively, our research reveals that the quorum sensing molecules AHLs boost OVA-specific IgE and IgG1 production via AKT-Rara interactions in DCs. AHLs may change DC phenotype as Th2 cells prime DCs (DC_{Th2}) with the following features: (1) hyporesponsiveness to TLR and (2) upregulated IFN-I signature, RA signature, and OX40L (Figure S5). Our research identifies the effect of a bacterial component on an allergic response and adds insight into the process of bacteria-induced IgE and IgG1 production. We have also demonstrated that when clinicians use specific bacterial strains to regulate allergic diseases (Niers et al., 2007; Toh et al., 2012), they should keep in mind the potential release of the quorum sensing molecules AHLs.

Limitations of the Study

There are several limitations of this study. First, we did not use the AHLs KO strain of *P. aeruginosa* in this study. Second, CD11c cre- Rara$^{fl/fl}$ mice were used as littermate controls, and we did not add CD11c cre + RARA$^{wt/wt}$ mice as controls.

Resource Availability

Lead Contact

Further information should be directed to the Lead Contact, Zongde Zhang (zongdez@swmu.edu.cn).

Materials Availability

Materials in this study are available from the Lead Contact upon reasonable request.

Data and Code Availability

Raw sequencing data were deposited in the NCBI Sequence Read Archive (SRA) under Project Accession: PRJNA631431.

METHODS

All methods can be found in the accompanying Transparent Methods supplemental file.

SUPPLEMENTAL INFORMATION

Supplemental Information can be found online at https://doi.org/10.1016/j.isci.2020.101288.

ACKNOWLEDGMENTS

We thank Dr. Yan Li of the Model Animal Research Center, Nanjing University, for insightful comments and critiques. We thank Xing Wang of the Affiliated Hospital of Southwest Medical University for technical assistance. This work was supported by the Fundamental Research Funds for the Central Universities (090314380026), the PI start-up funding from Model Animal Research Center, Nanjing University, open-funding from Key Laboratory of Allergy and Immunology, Shenzhen University, and Shenzhen Science and Technology Peacock Team Project (No. KQTD20170331145453160), the Foundation of Luzhou Science and Technology Program and Southwest Medical University (no.2019LZXNYDJ33), the Natural Science Foundation of Southwest Medical University (no.2018-ZRQN-034 and no.2019ZQN078), and PhD Research Startup Foundation of The Affiliated Hospital of Southwest Medical University (no.18053 and no.18076).

AUTHOR CONTRIBUTIONS

Z.Z. conceived the study and wrote the manuscript. R.W., Z.Z., N.M., X.L., X.J., and X.Y. performed the experiments. C.Q. helped with qPCR data analysis. H.T. helped with mouse experiment. Z.L. helped with manuscript writing and data discussion.

DECLARATION OF INTERESTS

The authors declare no competing interests.

Received: September 20, 2019
Revised: March 24, 2020
Accepted: June 14, 2020
Published: July 24, 2020

REFERENCES

Bachus, H., Kaur, K., Papillion, A.M., Marquez-Lago, T.T., Yu, Z., Ballesteros-Tato, A., Matalon, S., and Leon, B. (2019). Impaired tumor-necrosis-factor-alpha-driven dendritic cell activation limits lipopolysaccharide-induced protection from allergic inflammation in infants. Immunity *50*, 225–240.e4.

Bhattacharya, N., Yuan, R., Prestwood, T.R., Penny, H.L., DiMaio, M.A., Reticker-Flynn, N.E., Krois, C.R., Kenkel, J.A., Pham, T.D., Carmi, Y., et al. (2016). Normalizing microbiota-induced retinoic acid deficiency stimulates protective CD8(+) T cell-mediated immunity in colorectal cancer. Immunity *45*, 641–655.

Bisgaard, H., Li, N., Bonnelykke, K., Chawes, B.L., Skov, T., Paludan-Muller, G., Stokholm, J., Smith, B., and Krogfelt, K.A. (2011). Reduced diversity of the intestinal microbiota during infancy is associated with increased risk of allergic disease at school age. J. Allergy Clin. Immunol. *128*, 646–652.e1-5.

Cait, A., Hughes, M.R., Antignano, F., Cait, J., Dimitriu, P.A., Maas, K.R., Reynolds, L.A., Hacker, L., Mohr, J., Finlay, B.B., et al. (2018). Microbiome-driven allergic lung inflammation is ameliorated by short-chain fatty acids. Mucosal Immunol. *11*, 785–795.

Chen, C., Perry, T.L., Chitko-McKown, C.G., Smith, A.D., Cheung, L., Beshah, E., Urban, J.F., Jr., and Dawson, H.D. (2019). The regulatory actions of retinoic acid on M2 polarization of porcine macrophages. Dev. Comp. Immunol. *98*, 20–33.

Clarke, C.W., Hampshire, P., and Hannant, C. (1981). Positive immediate skin tests in cystic fibrosis: a possible role for Pseudomonas infection. Br. J. Dis. Chest *75*, 15–21.

Cleland, E.J., Bassiouni, A., and Wormald, P.J. (2013). The bacteriology of chronic rhinosinusitis and the pre-eminence of Staphylococcus aureus in revision patients. Int. Forum Allergy Rhinol. *3*, 642–646.

Connor, L.M., Tang, S.C., Cognard, E., Ochiai, S., Hilligan, K.L., Old, S.I., Pellefigues, C., White, R.F., Patel, D., Smith, A.A., et al. (2017). Th2 responses are primed by skin dendritic cells with distinct transcriptional profiles. J. Exp. Med. *214*, 125–142.

Dawson, H.D., Collins, G., Pyle, R., Key, M., and Taub, D.D. (2008). The Retinoic Acid Receptor-alpha mediates human T-cell activation and Th2 cytokine and chemokine production. BMC Immunol. *9*, 16.

Duan, W., So, T., and Croft, M. (2008). Antagonism of airway tolerance by endotoxin/lipopolysaccharide through promoting OX40L and suppressing antigen-specific Foxp3+ T regulatory cells. J. Immunol. *181*, 8650–8659.

Flynn, S., Toellner, K.M., Raykundalia, C., Goodall, M., and Lane, P. (1998). CD4 T cell cytokine differentiation: the B cell activation molecule, OX40 ligand, instructs CD4 T cells to express interleukin 4 and upregulates expression of the chemokine receptor, Blr-1. J. Exp. Med. *188*, 297–304.

Fyhrquist, N., Ruokolainen, L., Suomalainen, A., Lehtimaki, S., Veckman, V., Vendelin, J., Karisola, P., Lehto, M., Savinko, T., Jarva, H., et al. (2014). Acinetobacter species in the skin microbiota protect against allergic sensitization and inflammation. J. Allergy Clin. Immunol. *134*, 1301–1309.e1.

Galvin, K.C., Dyck, L., Marshall, N.A., Stefanska, A.M., Walsh, K.P., Moran, B., Higgins, S.C., Dungan, L.S., and Mills, K.H. (2013). Blocking retinoic acid receptor-alpha enhances the efficacy of a dendritic cell vaccine against tumours by suppressing the induction of regulatory T cells. Cancer Immunol. Immunother. *62*, 1273–1282.

Gao, Y., Nish, S.A., Jiang, R., Hou, L., Licona-Limon, P., Weinstein, J.S., Zhao, H., and Medzhitov, R. (2013). Control of T helper 2 responses by transcription factor IRF4-dependent dendritic cells. Immunity *39*, 722–732.

Gould, H.J., and Sutton, B.J. (2008). IgE in allergy and asthma today. Nat. Rev. Immunol. *8*, 205–217.

Hall, J.A., Cannons, J.L., Grainger, J.R., Dos Santos, L.M., Hand, T.W., Naik, S., Wohlfert, E.A., Chou, D.B., Oldenhove, G., Robinson, M., et al. (2011a). Essential role for retinoic acid in the promotion of CD4(+) T cell effector responses via retinoic acid receptor alpha. Immunity *34*, 435–447.

Hall, J.A., Grainger, J.R., Spencer, S.P., and Belkaid, Y. (2011b). The role of retinoic acid in tolerance and immunity. Immunity *35*, 13–22.

Homma, Y., Cao, S., Shi, X., and Ma, X. (2007). The Th2 transcription factor c-Maf inhibits IL-12p35 gene expression in activated macrophages by targeting NF-kappaB nuclear translocation. J. Interferon Cytokine Res. *27*, 799–808.

Huang, Y.J., and Boushey, H.A. (2015). The microbiome in asthma. J. Allergy Clin. Immunol. *135*, 25–30.

Huang, Y.J., Nelson, C.E., Brodie, E.L., Desantis, T.Z., Baek, M.S., Liu, J., Woyke, T., Allgaier, M., Bristow, J., Wiener-Kronish, J.P., et al. (2011). Airway microbiota and bronchial hyperresponsiveness in patients with suboptimally controlled asthma. J. Allergy Clin. Immunol. *127*, 372–381.e1-3.

Ito, T., Wang, Y.H., Duramad, O., Hori, T., Delespesse, G.J., Watanabe, N., Qin, F.X., Yao, Z., Cao, W., and Liu, Y.J. (2005). TSLP-activated dendritic cells induce an inflammatory T helper type 2 cell response through OX40 ligand. J. Exp. Med. *202*, 1213–1223.

Janss, T., Mesnil, C., Pirottin, D., Lemaitre, P., Marichal, T., Bureau, F., and Desmet, C.J. (2016). Interferon response factor-3 promotes the pro-Th2 activity of mouse lung CD11b(+) conventional dendritic cells in response to house dust mite allergens. Eur. J. Immunol. *46*, 2614–2628.

Joung, S.M., Park, Z.Y., Rani, S., Takeuchi, O., Akira, S., and Lee, J.Y. (2011). Akt contributes to activation of the TRIF-dependent signaling pathways of TLRs by interacting with TANK-binding kinase 1. J. Immunol. *186*, 499–507.

Kaisar, M.M.M., Ritter, M., Del Fresno, C., Jonasdottir, H.S., van der Ham, A.J., Pelgrom, L.R., Schramm, G., Layland, L.E., Sancho, D., Prazeres da Costa, C., et al. (2018). Dectin-1/2-induced autocrine PGE2 signaling licenses dendritic cells to prime Th2 responses. PLoS Biol. *16*, e2005504.

Khajanchi, B.K., Kirtley, M.L., Brackman, S.M., and Chopra, A.K. (2011). Immunomodulatory and protective roles of quorum-sensing signaling molecules N-acyl homoserine lactones during infection of mice with Aeromonas hydrophila. Infect. Immun. *79*, 2646–2657.

Kim, Y.G., Udayanga, K.G., Totsuka, N., Weinberg, J.B., Nunez, G., and Shibuya, A. (2014). Gut dysbiosis promotes M2 macrophage polarization and allergic airway inflammation via fungi-induced PGE(2). Cell Host Microbe *15*, 95–102.

Kravchenko, V.V., Kaufmann, G.F., Mathison, J.C., Scott, D.A., Katz, A.Z., Grauer, D.C., Lehmann, M., Meijler, M.M., Janda, K.D., and Ulevitch, R.J. (2008). Modulation of gene expression via disruption of NF-kappaB signaling by a bacterial small molecule. Science *321*, 259–263.

Lambrecht, B.N., and Hammad, H. (2017). The immunology of the allergy epidemic and the hygiene hypothesis. Nat. Immunol. *18*, 1076–1083.

Lee, J.Y., Ye, J., Gao, Z., Youn, H.S., Lee, W.H., Zhao, L., Sizemore, N., and Hwang, D.H. (2003). Reciprocal modulation of Toll-like receptor-4 signaling pathways involving MyD88 and phosphatidylinositol 3-kinase/AKT by saturated and polyunsaturated fatty acids. J. Biol. Chem. *278*, 37041–37051.

Lee, R.J., Xiong, G., Kofonow, J.M., Chen, B., Lysenko, A., Jiang, P., Abraham, V., Doghramji, L., Adappa, N.D., Palmer, J.N., et al. (2012). T2R38 taste receptor polymorphisms underlie susceptibility to upper respiratory infection. J. Clin. Invest. *122*, 4145–4159.

Li, N., Qiu, R., Yang, Z., Li, J., Chung, K.F., Zhong, N., and Zhang, Q. (2017). Sputum microbiota in severe asthma patients: relationship to eosinophilic inflammation. Respir. Med. *131*, 192–198.

Lovett-Racke, A.E., and Racke, M.K. (2002). Retinoic acid promotes the development of Th2-like human myelin basic protein-reactive T cells. Cell Immunol. *215*, 54–60.

Michel, O., Kips, J., Duchateau, J., Vertongen, F., Robert, L., Collet, H., Pauwels, R., and Sergysels, R. (1996). Severity of asthma is related to endotoxin in house dust. Am. J. Respir. Crit. Care Med. *154*, 1641–1646.

Miyairi, S., Tateda, K., Fuse, E.T., Ueda, C., Saito, H., Takabatake, T., Ishii, Y., Horikawa, M., Ishiguro, M., Standiford, T.J., and Yamaguchi, K. (2006). Immunization with 3-oxododecanoyl-L-homoserine lactone-protein conjugate protects mice from lethal Pseudomonas aeruginosa lung infection. J. Med. Microbiol. *55*, 1381–1387.

Niers, L.E., Hoekstra, M.O., Timmerman, H.M., van Uden, N.O., de Graaf, P.M., Smits, H.H., Kimpen, J.L., and Rijkers, G.T. (2007). Selection of probiotic bacteria for prevention of allergic diseases: immunomodulation of neonatal dendritic cells. Clin. Exp. Immunol. *149*, 344–352.

Ohshima, Y., Yang, L.P., Uchiyama, T., Tanaka, Y., Baum, P., Sergerie, M., Hermann, P., and Delespesse, G. (1998). OX40 costimulation enhances interleukin-4 (IL-4) expression at priming and promotes the differentiation of naive human CD4(+) T cells into high IL-4-producing effectors. Blood *92*, 3338–3345.

Okuda, J., Hayashi, N., Okamoto, M., Sawada, S., Minagawa, S., Yano, Y., and Gotoh, N. (2010). Translocation of Pseudomonas aeruginosa from the intestinal tract is mediated by the binding of ExoS to an Na,K-ATPase regulator, FXYD3. Infect. Immun. *78*, 4511–4522.

Park, D., Lapteva, N., Seethammagari, M., Slawin, K.M., and Spencer, D.M. (2006). An essential role for Akt1 in dendritic cell function and tumor immunotherapy. Nat. Biotechnol. *24*, 1581–1590.

Passador, L., Cook, J.M., Gambello, M.J., Rust, L., and Iglewski, B.H. (1993). Expression of Pseudomonas aeruginosa virulence genes requires cell-to-cell communication. Science *260*, 1127–1130.

Pitcher-Wilmott, R.W., Levinsky, R.J., Gordon, I., Turner, M.W., and Matthew, D.J. (1982). Pseudomonas infection, allergy, and cystic fibrosis. Arch. Dis. Child *57*, 582–586.

Pollara, G., Handley, M.E., Kwan, A., Chain, B.M., and Katz, D.R. (2006). Autocrine type I interferon amplifies dendritic cell responses to lipopolysaccharide via the nuclear factor-kappaB/p38 pathways. Scand. J. Immunol. *63*, 151–154.

Rodriguez, M.J., Aranda, A., Fernandez, T.D., Cubells-Baeza, N., Torres, M.J., Gomez, F., Palomares, F., Perkins, J.R., Rojo, J., Diaz-Perales, A., and Mayorga, C. (2017). LPS promotes Th2 dependent sensitisation leading to anaphylaxis in a Pru p 3 mouse model. Sci. Rep. *7*, 40449.

Savage, J.H., Lee-Sarwar, K.A., Sordillo, J., Bunyavanich, S., Zhou, Y., O'Connor, G., Sandel, M., Bacharier, L.B., Zeiger, R., Sodergren, E., et al. (2018). A prospective microbiome-wide association study of food sensitization and food allergy in early childhood. Allergy *73*, 145–152.

Schuijs, M.J., Willart, M.A., Vergote, K., Gras, D., Deswarte, K., Ege, M.J., Madeira, F.B., Beyaert, R., van Loo, G., Bracher, F., et al. (2015). Farm dust and endotoxin protect against allergy through A20 induction in lung epithelial cells. Science *349*, 1106–1110.

Skalski, J.H., Limon, J.J., Sharma, P., Gargus, M.D., Nguyen, C., Tang, J., Coelho, A.L., Hogaboam, C.M., Crother, T.R., and Underhill, D.M. (2018). Expansion of commensal fungus Wallemia mellicola in the gastrointestinal mycobiota enhances the severity of allergic airway disease in mice. PLoS Pathog. *14*, e1007260.

Smits, H.H., Hiemstra, P.S., Prazeres da Costa, C., Ege, M., Edwards, M., Garn, H., Howarth, P.H., Jartti, T., de Jong, E.C., Maizels, R.M., et al. (2016). Microbes and asthma: opportunities for intervention. J. Allergy Clin. Immunol. *137*, 690–697.

Son, A., Oshio, T., Kawamura, Y.I., Hagiwara, T., Yamazaki, M., Inagaki-Ohara, K., Okada, T., Wu, P., Iseki, M., Takaki, S., et al. (2013). TWEAK/Fn14 pathway promotes a T helper 2-type chronic colitis with fibrosis in mice. Mucosal Immunol. *6*, 1131–1142.

Song, D., Meng, J., Cheng, J., Fan, Z., Chen, P., Ruan, H., Tu, Z., Kang, N., Li, N., Xu, Y., et al. (2019). Pseudomonas aeruginosa quorum-sensing metabolite induces host immune cell death through cell surface lipid domain dissolution. Nat. Microbiol. *4*, 97–111.

Srinivas, H., Xia, D., Moore, N.L., Uray, I.P., Kim, H., Ma, L., Weigel, N.L., Brown, P.H., and Kurie, J.M. (2006). Akt phosphorylates and suppresses the transactivation of retinoic acid receptor alpha. Biochem. J. *395*, 653–662.

Stoodley, B.J., and Thom, B.T. (1970). Observations on the intestinal carriage of Pseudomonas aeruginosa. J. Med. Microbiol. *3*, 367–375.

Strachan, D.P. (1989). Hay fever, hygiene, and household size. BMJ *299*, 1259–1260.

Tang, H.B., DiMango, E., Bryan, R., Gambello, M., Iglewski, B.H., Goldberg, J.B., and Prince, A. (1996). Contribution of specific Pseudomonas aeruginosa virulence factors to pathogenesis of pneumonia in a neonatal mouse model of infection. Infect. Immun. *64*, 37–43.

Telford, G., Wheeler, D., Williams, P., Tomkins, P.T., Appleby, P., Sewell, H., Stewart, G.S., Bycroft, B.W., and Pritchard, D.I. (1998). The Pseudomonas aeruginosa quorum-sensing signal molecule N-(3-oxododecanoyl)-L-homoserine lactone has immunomodulatory activity. Infect. Immun. *66*, 36–42.

Toh, Z.Q., Anzela, A., Tang, M.L., and Licciardi, P.V. (2012). Probiotic therapy as a novel approach for allergic disease. Front. Pharmacol. *3*, 171.

Trinchieri, G. (1994). Interleukin-12: a cytokine produced by antigen-presenting cells with immunoregulatory functions in the generation of T-helper cells type 1 and cytotoxic lymphocytes. Blood *84*, 4008–4027.

Vellozo, N.S., Pereira-Marques, S.T., Cabral-Piccin, M.P., Filardy, A.A., Ribeiro-Gomes, F.L., Rigoni, T.S., DosReis, G.A., and Lopes, M.F. (2017). All-trans retinoic acid promotes an M1- to M2-phenotype shift and inhibits macrophage-mediated immunity to Leishmania major. Front. Immunol. *8*, 1560.

Webb, L.M., Lundie, R.J., Borger, J.G., Brown, S.L., Connor, L.M., Cartwright, A.N., Dougall, A.M., Wilbers, R.H., Cook, P.C., Jackson-Jones, L.H., et al. (2017). Type I interferon is required for T helper (Th) 2 induction by dendritic cells. EMBO J. *36*, 2404–2418.

Williams, J.W., Tjota, M.Y., Clay, B.S., Vander Lugt, B., Bandukwala, H.S., Hrusch, C.L., Decker, D.C., Blaine, K.M., Fixsen, B.R., Singh, H., et al. (2013). Transcription factor IRF4 drives dendritic cells to promote Th2 differentiation. Nat. Commun. *4*, 2990.

Zhang, Z., Adappa, N.D., Doghramji, L.J., Chiu, A.G., Cohen, N.A., and Palmer, J.N. (2015). Different clinical factors associated with Staphylococcus aureus and Pseudomonas aeruginosa in chronic rhinosinusitis. Int. Forum Allergy Rhinol. *5*, 724–733.

Zhang, Z., Li, J., Zheng, W., Zhao, G., Zhang, H., Wang, X., Guo, Y., Qin, C., and Shi, Y. (2016). Peripheral lymphoid volume expansion and maintenance are controlled by gut microbiota via RALDH+ dendritic cells. Immunity *44*, 330–342.

iScience, Volume *23*

Supplemental Information

Bacterial Quorum Sensing Molecules Promote Allergic Airway Inflammation by Activating the Retinoic Acid Response

Renlan Wu, Xingjie Li, Ning Ma, Xiufeng Jin, Xiefang Yuan, Chen Qu, Hongmei Tang, Zhigang Liu, and Zongde Zhang

Fig. S1

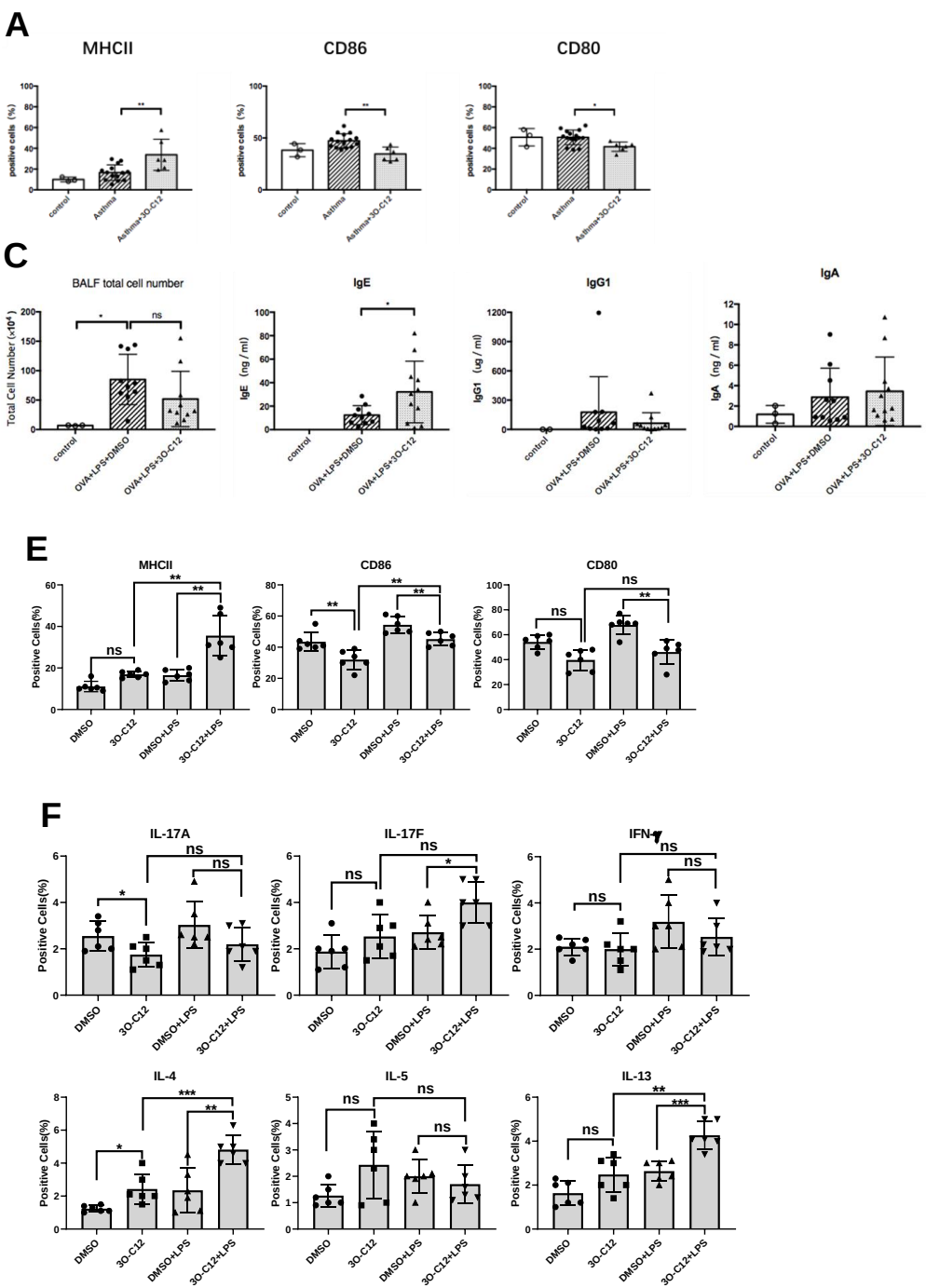
A
MHCII
CD86
CD80
positive cells (%)
control
Asthma
Asthma+3O-C12
B
IL-17A
IL-17F
IFN-γ
IL-4
IL-5
IL-13
C
BALF total cell number
Total Cell Number (×10⁴)
IgE
IgE (ng / ml)
IgG1
IgG1 (ug / ml)
IgA
IgA (ng / ml)
control
OVA+LPS+DMSO
OVA+LPS+3O-C12
D
IL-17A
IL-17F
IFN-γ
IL-4
IL-5
IL-13
control
OVA+LPS+DMSO
OVA+LPS+3O-C12
E
MHCII
CD86
CD80
Positive Cells(%)
DMSO
3O-C12
DMSO+LPS
3O-C12+LPS
F
IL-17A
IL-17F
IFN-γ
IL-4
IL-5
IL-13
Positive Cells(%)
DMSO
3O-C12
DMSO+LPS
3O-C12+LPS

Fig. S2

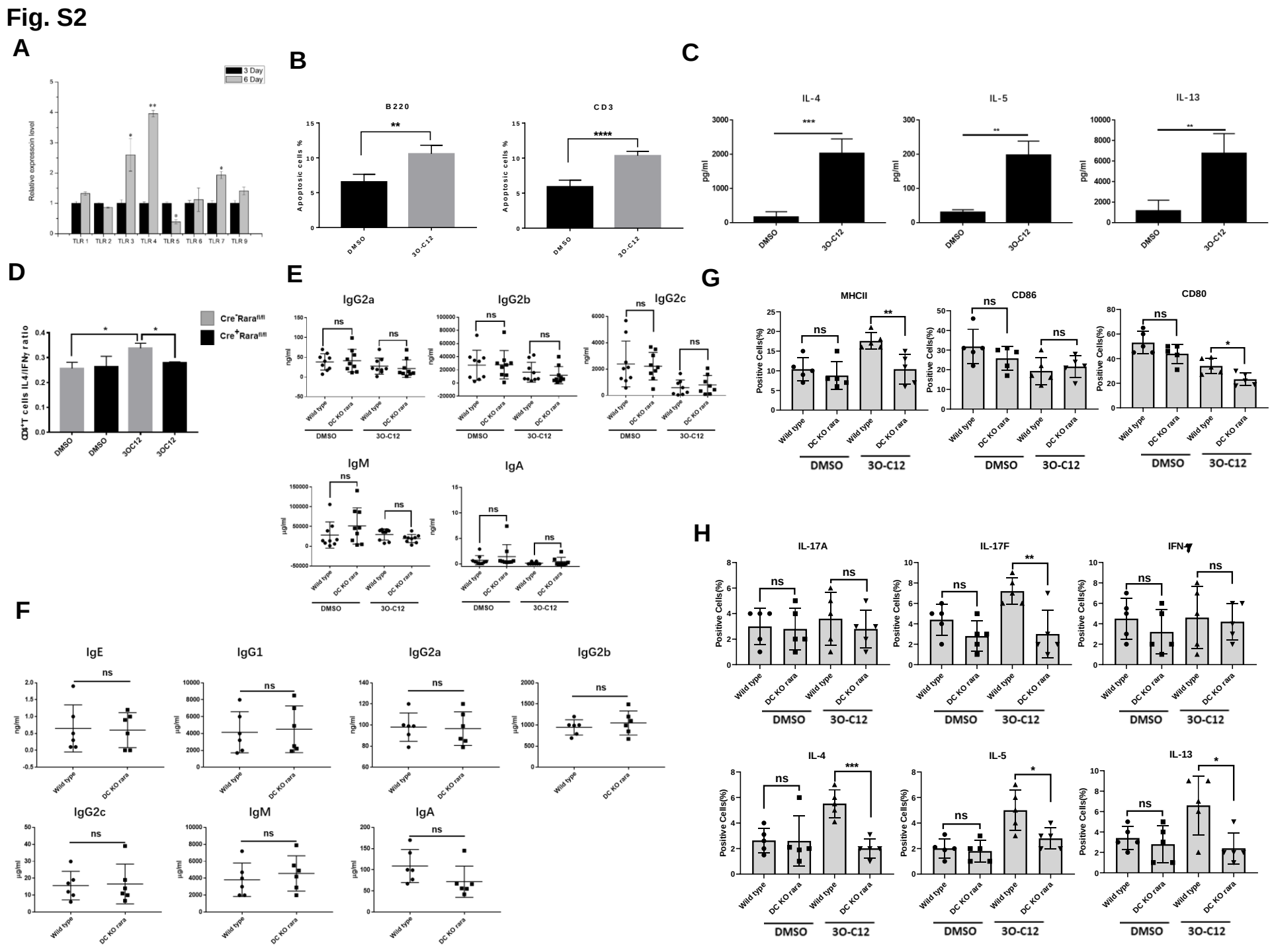
A
3 Day
6 Day
Relative expression level
TLR 1
TLR 2
TLR 3
TLR 4
TLR 5
TLR 6
TLR 7
TLR 9
B
B220
CD3
Apoptosic cells %
DMSO
3O-C12
C
IL-4
IL-5
IL-13
pg/ml
D
Cre-Rarafl/fl
Cre+Rarafl/fl
CD4+T cells IL4/IFNγ ratio
E
IgG2a
IgG2b
IgG2c
IgM
IgA
ng/ml
μg/ml
Wild type
DC KO rara
F
IgE
IgG1
G
MHCII
CD86
CD80
Positive Cells(%)
H
IL-17A
IL-17F
IFN-γ
IL-4
IL-5
IL-13
ns

Fig. S3

A

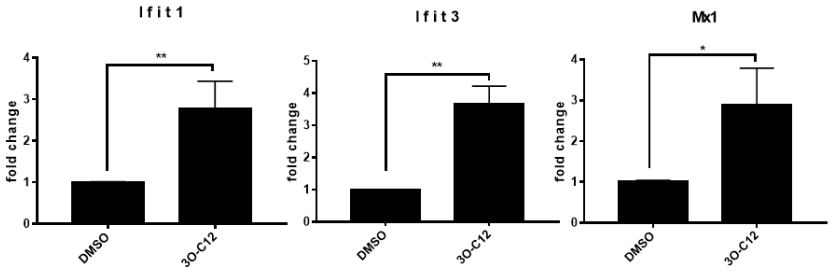

B

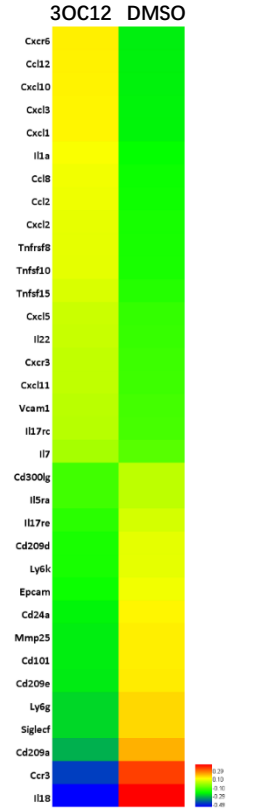

Chemokines&cytokines signature

C

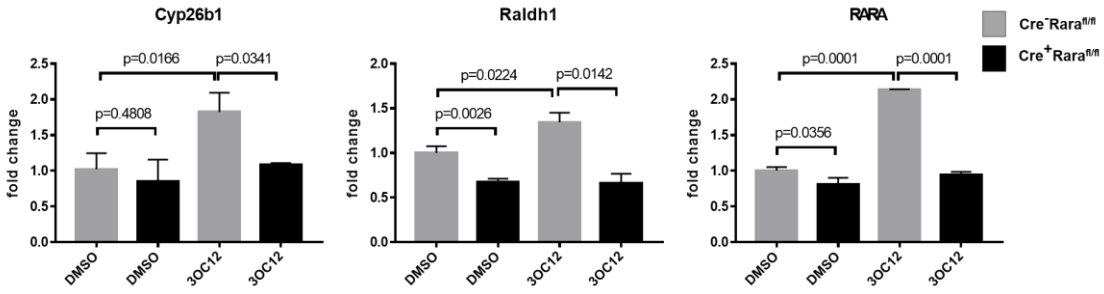

Fig. S4

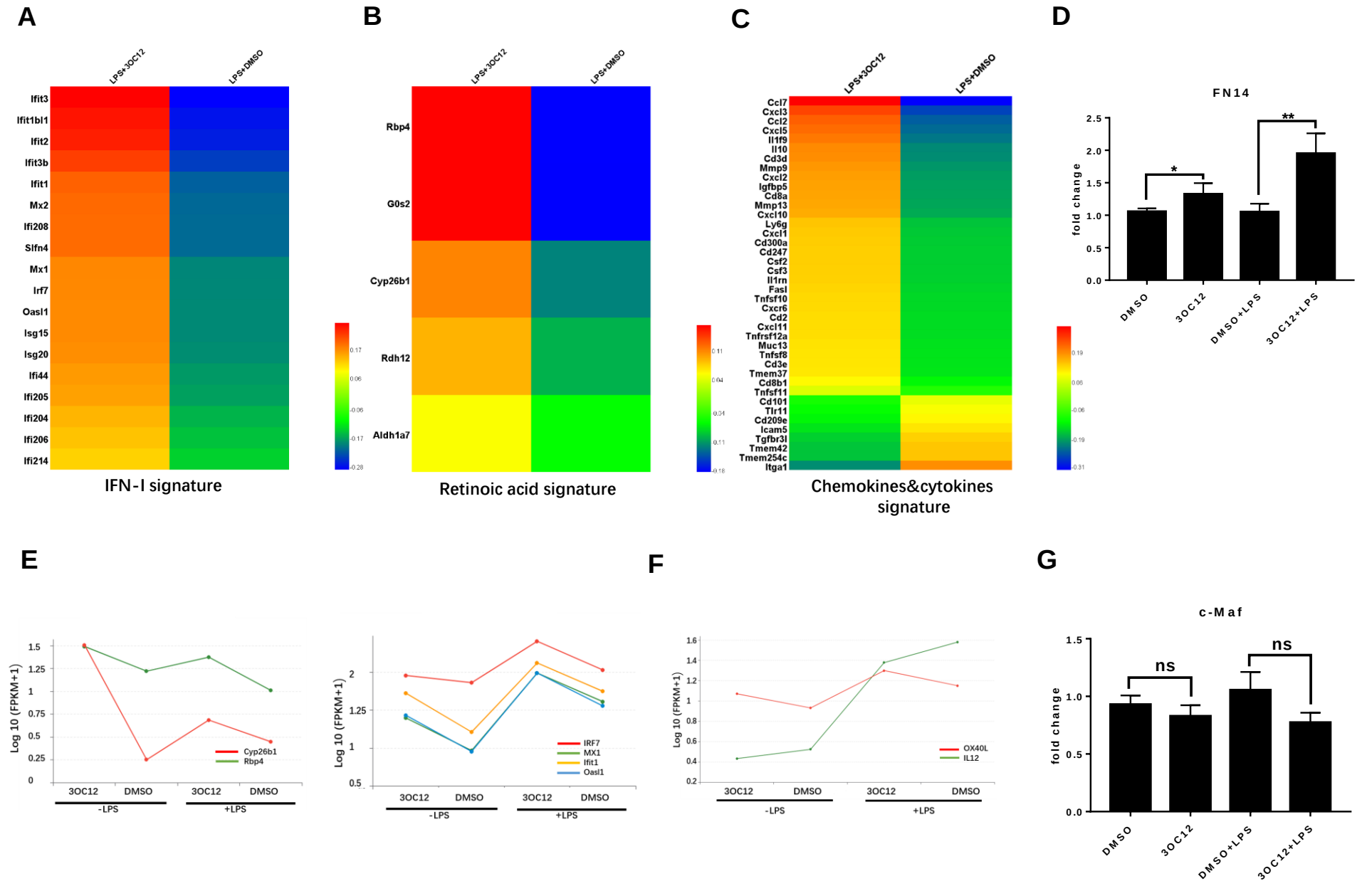
A
LPS+3OC12
LPS+DMSO
Ifit3
Ifit1bl1
Ifit2
Ifit3b
Ifit1
Mx2
Ifi208
Slfn4
Mx1
Irf7
Oasl1
Isg15
Isg20
Ifi44
Ifi205
Ifi204
Ifi206
Ifi214
IFN-I signature
B
LPS+3OC12
LPS+DMSO
Rbp4
G0s2
Cyp26b1
Rdh12
Aldh1a7
Retinoic acid signature
C
LPS+3OC12
LPS+DMSO
Ccl7
Cxcl3
Ccl2
Cxcl5
Il1f9
Il10
Cd3d
Mmp9
Cxcl2
Igfbp5
Cd8a
Mmp13
Cxcl10
Ly6g
Cxcl1
Cd300a
Cd247
Csf2
Csf3
Il1rn
Fasl
Tnfsf10
Cxcr6
Cd2
Cxcl11
Tnfrsf12a
Muc13
Tnfsf8
Cd3e
Tmem37
Cd8b1
Tnfsf11
Cd101
Tlr11
Cd209e
Icam5
Tgfbr3l
Tmem42
Tmem254c
Itga1
Chemokines&cytokines signature
D
FN14
fold change
DMSO
3OC12
DMSO+LPS
3OC12+LPS
E
Log 10 (FPKM+1)
Cyp26b1
Rbp4
3OC12
DMSO
-LPS
+LPS
Log 10 (FPKM+1)
IRF7
MX1
Ifit1
Oasl1
F
Log 10 (FPKM+1)
OX40L
IL12
G
c-Maf
fold change
ns
DMSO
3OC12
DMSO+LPS
3OC12+LPS

Fig. S5

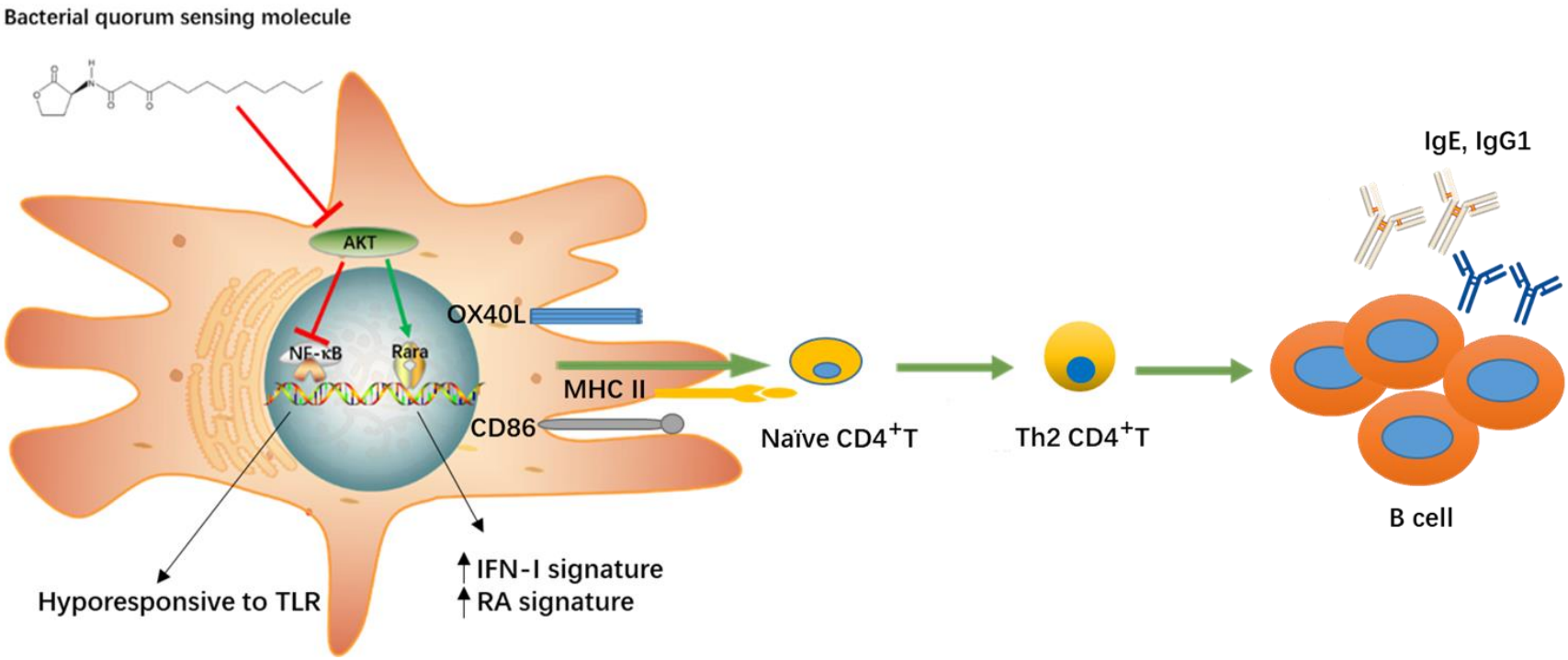
Bacterial quorum sensing molecule
AKT
NF-κB
Rara
OX40L
MHC II
CD86
Hyporesponsive to TLR
IFN-I signature
RA signature
Naïve CD4+T
Th2 CD4+T
IgE, IgG1
B cell

Table S1

Item	Name	Synonyms	Chemical structure
10007895	N-3-oxo-dodecanoyl-L-Homoserine lactone	3O-C12	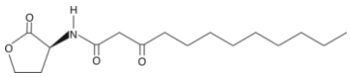
10011199	N-octanoyl-L-Homoserine lactone	C8	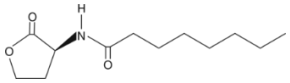
10011203	N-dodecanoyl-L-Homoserine lactone	C12	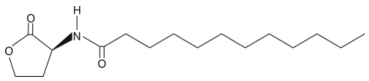
13209	N-octadecanoyl-L-Homoserine lactone	C18	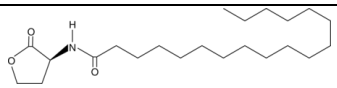
10011200	N-tetradecanoyl-L-Homoserine lactone	C14	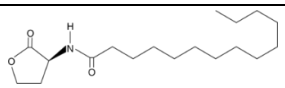
10007898	N-butyryl-L-Homoserine lactone	C4	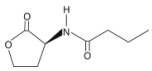
13063	N-3-oxo-tetradecanoyl-L-Homoserine lactone	3O-C14	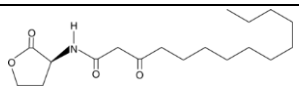
10007896	N-hexanoyl-L-Homoserine lactone	C6	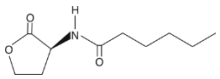
10011201	N-decanoyl-L-Homoserine lactone	C10	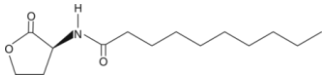
10011206	N-3-oxo-octanoyl-L-Homoserine lactone	3O-C8	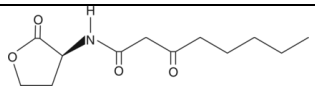
13062	N-3-oxo-hexadecanoyl-L-Homoserine lactone	3O-C16	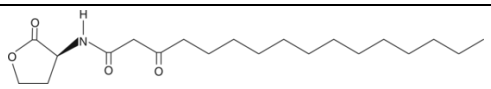
10011207	N-(β -ketocaproyl)-L-Homoserine lactone	3O-C6	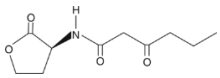
10011238	N-3-oxo-hexadec-11(Z)-enoyl-L-Homoserine lactone	3O-C16Δ	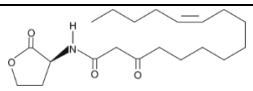

Table S1. Chemical structure of AHLs. Related to Figure 4.

Figure S1. 3O-C12 enhances allergic lung inflammation. Related to Figure 1.

(A) Balb/c mice were divided into three groups: control (n = 4), asthma (n = 15), and asthma + 3O-C12 (n = 6). The mice were intraperitoneally (i.p.) injected on day 1 and day 13 with OVA (50 μg) and aluminum hydroxide (2 mg). On day 20 and 22, the mice were intranasally (i.n.) challenged with OVA (40 μg) and i.p. administered with or without 3O-C12 (500 μg). On day 25, 27, and 29, the mice were i.n. challenged with OVA (40 μg) and i.n. administered with or without 3O-C12 (50 μg). One day after the last OVA challenge, mice were sacrificed. Expression of DC surface markers **(A)** and cytokines of $CD4^+$T **(B)** from spleen were determined by flow cytometry. Data are representative of three independent experiments

(C) BMDCs from C57BL/6 mice were stimulated by OVA (200 μg/ml) and LPS (100 ng/ml) overnight, with or without 3O-C12 (10 μM). BMDCs were transferred intranasally (i.n.) to recipients (C57BL/6 mice) (n = 3 in control group; n = 10 in OVA + LPS + DMSO group; n = 11 in OVA + LPS + 3O-C12 group) on days 1 and 12. Each recipient was challenged by 40 μg OVA i.n. on days 13, 14, and 15. One day after the last OVA challenge, mice were sacrificed and assessed for bronchoalveolar lavage fluid (BALF) total cell number **(C)**, serum immunoglobulins **(C)**, and $CD4^+$ T cell cytokine production from the spleen **(D)**.

(E−F) Wild-type C57BL/6 mice were subcutaneously immunized with OVA (50 μg/mouse) + LPS (0.5 μg/mouse) with or without 3O-C12 (250 μg/mouse) every week for three weeks; incomplete Freund adjuvant was used as a vehicle. Expression of DC surface markers **(E)** and cytokines of $CD4^+$T **(F)** from spleen were determined by flow cytometry. Results are representative of three independent experiments.

Data are presented as mean ± SD; p-values were calculated using the two-tailed Student's t-test. *$p < 0.05$, **$p < 0.01$, ***$p < 0.001$, ****$p < 0.0001$, n.s.: not significant.

Figure S2. 3O-C12-activated DCs induced CD4+T Th2 differentiation that depended on Rara. Related to Figure 1 and Figure 5.

(A) Quantitative real-time PCR analysis of the TLR expression pattern of BMDCs cultured for 3 and 6 d.

(B) Spleen cells cultured from C57BL/6 mice were incubated with 3O-C12 (10 μM) for 12 h, annexin v-positive cells gated on B220 and CD3 were determined by flow cytometry.

(C) OT-II cells were activated by 3O-C12-conditioned DCs in the presence of OVA antigen for 5 d and restimulated with anti-CD3 and anti-CD28 antibody for cytokine analysis.

(D) BMDCs (5−7 d) cultured from $CD11ccre^+Rara^{fl/fl}$ mice ($Cre+Rara^{fl/fl}$) and littermate control $CD11ccre^-Rara^{fl/fl}$ mice ($Cre-Rara^{fl/fl}$), were loaded with OVA (100 μg/mL) and incubated with LPS or LPS+3O-C12 (10 μM) for 1−3 h. Naive OT-II cells were added and co-cultured for 5 d. IL-4- and IFN-ɣ-positive cells were determined by flow cytometry.

(E) $CD11ccre^+Rara^{fl/fl}$ mice (DC KO Rara) and littermate control $CD11ccre^-Rara^{fl/fl}$ mice (wild-type) were subcutaneously immunized with OVA (50 μg/mouse) + LPS (0.5 μg/mouse) with or without 3O-C12 (250 μg/mouse) every week for three weeks. Mouse serum was collected and OVA-specific immunoglobulins were analyzed by ELISA.

(F) Basal levels of immunoglobulins in $CD11ccre^+Rara^{fl/fl}$ mice (DC KO Rara) and littmite control $CD11ccre^-Rara^{fl/fl}$ mice (wild-type) were analyzed by ELISA.

(G−H) $CD11ccre^+Rara^{fl/fl}$ mice (DC KO Rara) and littermate control $CD11ccre^-Rara^{fl/fl}$ mice (wild-type) were

subcutaneously immunized with OVA (50 μg/mouse) + LPS (0.5 μg/mouse) with or without 3O-C12 (250 μg/mouse) every week for three weeks. Expression of DC surface markers **(G)** and cytokines of $CD4^+$T cells **(H)** from spleen were determined by flow cytometry.

Data are representative of three independent experiments. Data are presented as mean ± SD; p-values were calculated using the two-tailed Student's t-test. *p < 0.05, **p < 0.01, ***p < 0.001, ****p < 0.0001, n.s.: not significant.

Figure S3. 3O-C12 upregulated multiple genes in DCs. Related to Figure 6.

(A) The IFN-I signature stimulated by 3O-C12 was examined with Q-PCR.

(B) RNA-seq analysis of chemokines and chemokine receptor gene expression of 3O-C12-activated DCs. Heatmap of FPKM values.

(C) The RA signature stimulated by 3O-C12 was dependent on Rara.

Data of Q-PCR are representative of three independent experiments. Data are presented as mean ± SD; p-values were calculated using the two-tailed Student's t-test. *p < 0.05, **p < 0.01, ***p < 0.001, ****p < 0.0001, n.s.: not significant.

Figure S4. LPS enhances the 3O-C12-stimulated expression of the IFN-I signature and OX40L. Related to Figure 6.

(A−E) RNA-seq analysis of the gene expression of 3O-C12 + LPS-activated DCs.

(A−C) Heatmap of FPKM values.

(D) Q-PCR analysis of FN14 (TNFRSF12A) expression in DCs.

(E) The expression level of the IFN-I and RA signature in 3O-C12-activated and 3O-C12+LPS-activated DCs.

(F) The expression level of IL12 and OX40L in 3O-C12-activated and 3O-C12+LPS-activated DCs.

(G) Q-PCR analysis of c-Maf expression in DCs.

Data of Q-PCR are representative of three independent experiments. Data are presented as mean ± SD; p-values were calculated using the two-tailed Student's t-test. *p < 0.05, **p < 0.01, ***p < 0.001, ****p < 0.0001, n.s.: not significant.

Figure S5. Graphical representation of the phenotype of 3O-C12-activated DCs. Related to Figure 1 and Figure 6.

Materials and Methods

Ethics Statement

All animal experiments were performed in accordance with the recommendations outlined in the Guide for the Care and Use of Laboratory Animals. All research animal protocols were approved by the Institutional Animal Care and Use Committee at the Model Animal Research Center, Nanjing University (animal protocol number: AP#ZZD01)

Reagents

Acyl-homoserine lactone molecules (Table S1) were purchased from Cayman Chemical Company (Ann Arbor, USA), dissolved in DMSO, and stored at -20 ℃. TLR1-9 ligands used for stimulation of DCs were purchased from Invivogen. T2R38 receptor agonists 6PTU (6-n-propylthiouracil) and NP (N-Phenylthiourea), phospholipase C inhibitor U73122, and OVA were purchased from Sigma. DDAOG was purchased from Invitrogen and recombinant mouse IGF-1 and PDGF from R&D or Genscript.

Mice

The Tg(RARE-Hspa1b/lacZ)12Jrt/J strain was obtained from Jackson Laboratories and maintained as homozygotes to retain the reporter activity. $CD11c^{cre}$ and OT-II mice with a C57BL/6 background were purchased from Jackson Laboratories. $Rara^{fl/fl}$ mice were established in our lab as previously reported. C57BL/6 was purchased from the Nanjing Biomedical Research Institute of the Nanjing University. All research animal

protocols were approved by the Institutional Animal Care and Use Committee of the Model Animal Research Center, Nanjing University.

FACS and antibody

DCs were washed and suspended in FACS buffer (PBS, 2% FBS), incubated with fluorochrome-coupled agents for 30 min at 4 ℃, and then washed in FACS buffer. Data were obtained with the Accuri C6 Flow Cytometer (BD Biosciences) and analyzed by FlowJo software v9.6 (FlowJo, Ashland, USA). The following anti-murine antibodies were used for flow cytometric analysis: CD40 (HM40-3), CD80 (16-10A1), CD86 (GL1), ICAM1 (YN1/1.7.4), CD11c (N418), TCR V alpha 2 (B20.1), IL-4 (11B11), CD4 (RM4-5), B220 (RA3-6B2), CD3 (17A2) (all purchased from eBioscience), MHCII (M5/114.15.2), OX40L(RM134L), and IFN-ɣ (XMG1.2) (Biolegend).

BMDC culture and isolation of spleen DCs

DCs were generated from bone marrow (BM) cells obtained from 5–7-week-old, female and male RA reporter mice or C57BL/6 mice. Briefly, BM cells were flushed out from femurs and tibias. BM cells were cultured in complete culture medium (RPMI 1640 supplemented with 10% FBS, 25 mM HEPES, 5 mM 2-ME, and antibiotics; Hyclone) containing 10 ng/ml GM-CSF and 10 ng/ml IL-4 (Peprotech). Spleen DCs were isolated with magnetic-activated cell sorting (MACS) by EasySep™ Mouse CD11c Positive Selection Kit (stem cell), according to the manufacturer's instructions.

Adoptive transfer of BMDCs

Bone marrow (BM) cells were harvested from femurs and tibiae of 5-week-old, female and male C57BL/6 mice and cultured in complete culture medium (RPMI 1640 supplemented with 10% FBS, 25 mM HEPES, 5 mM 2-ME, antibiotics, and 10 ng/ml mouse GM-CSF and IL-4) for 7 days, and then BMDCs were harvested from floating cells. BMDCs were stimulated by OVA (200 μg/ml) and LPS (100 ng/ml) overnight, with or without 3O-C12 (10 μM). Then, BMDCs were washed and resuspended in PBS. BMDCs (5×10^5) in 20 μl were transferred intranasally (i.n.) to recipients (C57/B6 mice, male) (n = 3 in control group (not treated); n = 10 in OVA + LPS + DMSO-treated BMDC transfer group; n = 11 in OVA + LPS + 3O-C12-treated BMDC transfer group) on days 1 and 12. Each recipient was challenged with 40 μg OVA i.n. on days 13, 14, and 15. One day after the last OVA challenge, mice were sacrificed and the following was assessed: bronchoalveolar lavage fluid (BALF) total cell number and eosinophil number, lung histology, serum immunoglobulins, DC surface marker expression, and $CD4^+$ T cell cytokine production.

Mouse model of asthma

Balb/c mice (6 weeks of age, male) were divided into three groups: control (not treated) (n=4), asthma (n=15), and asthma + 3O-C12 group (n=6). They were intraperitoneally (i.p.) injected on day 1 and day 13 with OVA (50 μg, Sigma) and aluminum hydroxide (2 mg, Sigma). On day 20 and 22, the mice were i.n. challenged with OVA (40 μg) and i.p. administered with or without 3O-C12 (500 μg). On day 25, 27, and 29, the mice were i.n. challenged with OVA (40 μg) and i.n. administered with or without 3O-C12

(500 μg). One day after the last OVA challenge, mice were sacrificed and the following was assessed: bronchoalveolar lavage fluid (BALF) total cell number and eosinophil number, lung histology, serum immunoglobulins, DC surface marker expression, and $CD4^+$ T cell cytokine production.

Multiple cytokine detection

Cytokines were measured by MILLIPLEX® Multiplex Assays using a Luminex 100 platform (Luminex, Austin, TX) and BioManager software (Bio-Rad, Hercules, CA) for analysis. The following multiplexing kits were purchased from Millipore (Billerica, MA): Mouse Cytokine/Chemokine Panel III, containing IL-20, IL-23, IL-27, IL-33, CCL22, and TIMP-1. Kits were used according to the manufacturer's instructions.

Enzyme-linked immunosorbent assay (ELISA)

Cell supernatants were collected 24 h after exposure to 3O-C12. Levels of the cytokines IL-6 and TNF-α (R&D Systems, Minneapolis, USA) were measured by ELISA kits according to the manufacturer's instructions. Mouse serum was collected after the last immunization, levels of total and OVA-specific IgE, IgG1, IgG2a, IgG2c, IgM, IgA, and IgG2b were determined by ELISA. Briefly, OVA was coated in coating buffer (Biolegend). After washing and blocking, diluted serum samples were added, and then primary antibodies against OVA-specific immunoglobulin (Chondrex) were added. After washing, HRP-labeled secondary antibodies (Southern Biotech) were added, TMB Reagent (Biolegend) was used for color development, and optical density was read at 450 nm.

β-galactosidase activity

spDCs and BMDCs from female and male RA reporter mice were incubated with DDAOG (10 μM) in serum-free Hank's buffer for 30 min to 2 h at 37 °C. The cells were washed three times with Hank's buffer before flow cytometry analysis. Upon excitation, DDAO generates a far-red-shifted fluorescent signal that can be detected by flow cytometry.

Western blots

DCs were collected and lysed on ice with RIPA Buffer (CST) containing Protease/Phosphatase Inhibitor Cocktail (CST) and 1 mM PMSF (CST). Cell extracts were loaded onto Biofuraw™ Precast Gel (Tanon), separated by electrophoresis, and transferred onto NC membranes (Millipore). Signals were generated with High-sig ECL Western Blotting Substrate (Tanon). The antibodies were all purchased from CST company: anti-GSK-3β (27C10) rabbit mAb, anti-Phospho-GSK-3β (Ser9) (5B3) rabbit mAb, anti-Phospho-AKT (Ser473) (D9E) XP® rabbit mAb, anti-AKT (pan) (C67E7) rabbit mAb, anti-GAPDH (14C10) rabbit mAb, and NF-κB Pathway Sampler Kit. Band signals were quantified with the ImageJ software and analyzed with the GraphPad Prism software.

DC/T-cell co-culture assays

BMDCs were isolated by EasySep™ Mouse CD11c Positive Selection Kit (stem cell), according to the manufacturer's instructions, loaded with OVA (200 μg/ml), then mixed

with CD62Lhi/CD44low naive CD4+OT-II T-cells (DC/T cell ratio 1:4) isolated with EasySep mouse CD4+T-cell enrichment kit (StemCell), and co-cultured for six days. Differentiation of Th1-Th2 was determined by FACS analysis of intracellular staining of IL4 and IFN- ɣ in activated CD4+OT-II T-cells.

RNA isolation, library construction, and sequencing

Total RNA from DCs was extracted using the TRIzol Reagent (Invitrogen) according to the manufacturer's protocol. Poly (A)+ RNA was purified from 5 μg of pooled total RNA using oligo(dT) magnetic beads, sheared into short fragments, and primed for cDNA library synthesis using the TruSeq RNA sample preparation kit per Illumina protocol. After quantitation using a TBS-380 mini-fluorometer (PicoGreen), the samples were clustered (TruSeq paired-end cluster kit, v3-cBot-HS; Illumina) and sequenced on the HiSeq2000 platform (100 bp, TruSeq SBS kit v3-HS 200 cycles; Illumina). Annotations for the entire data set were obtained with Tophat and followed by statistical analysis with Cufflink (Cuffdiff module). The read counts were further normalized into FPKM (Fragments Per Kilobases per Million reads). The FPKM values from the libraries were pairwise compared, and the fold changes were calculated by using RSEM software (version 1.2.7), and DEGs were identified by using the DESeq2 or edgeR software package (version 3.8.2) (if $P < 0.05$ and FDR < 0.05, the result was considered statistically significant). The data were analyzed on the free online platform of Majorbio I-Sanger Cloud Platform (www.i-sanger.com). The heat maps were generated by HemI (Heatmap Illustrator) software from the collected gene ($P < 0.05$).

Quantitative Real-Time PCR

BMDC cDNA was synthesized from 2 mg of total RNA by the Superscript III reverse transcription system (Invitrogen). qPCR was performed with SYBR green PCR mix and StepOnePlus machine (Applied Biosystems). PCR primers of mouse genes were purchased from OriGene. Gapdh was used as an internal control.

Statistical analysis

Statistical analysis was performed with the SPSS statistical software version 13.0 (SPSS Inc., Chicago). All plot graphs show means with standard deviation (SD). Statistical significance was determined with the two-tailed Student's t-test. A p-value of less than 0.05 was considered statistically significant. *$p < 0.05$, **$p < 0.01$, ***$p < 0.001$, not significant (N.S.). Data that did not exhibit a normal distribution were analyzed using the nonparametric Kruskal-Wallis test with Dunn's post hoc test.